Image Cover Sheet

CLASSIFICATION	SYSTEM NUMBER
UNCLASSIFIED	58364

TITLE

RADON TRANSFORM TECHNIQUES FOR WAKE DETECTION IN SAR \(SYNTHETIC APERTURE RADAR\) IMAGES

System Number:

Patron Number:

Requester:

Notes:

DSIS Use only:

Deliver to: JR

88-661

ROY BALL ASSOCIATES LTD.

SYSTEMS ENGINEERING

EVISION	DESCRIPTION	BY	APPROVED	DATE

TITLE:

RADON TRANSFORM TECHNIQUES FOR WAKE DETECTION IN SAR IMAGES

FOR: Defence Research Establishment, Ottawa

BY: ROY BALL ASSOCIATES LTD.
1750 Courtwood Crescent
Ottawa, Ontario
CANADA

DATE: March 31, 1988
CONTRACT: C250

J M Forlinsbee 30/Mar/88
RIGINATOR DATE

L O Ball 31 Mar 88
ROJECT MANAGER DATE

ICE-PRESIDENT ENGINEERING DATE

DOCUMENT NUMBER

FR-C250-000-0000

TABLE OF CONTENTS

		Page
ABSTRACT		
SUMMARY		-i-
1.0	**INTRODUCTION**	1
1.1	SHIP WAKES	1
1.2	SYNTHETIC APERTURE RADAR	1
1.3	RADON TRANSFORM	2
1.4	IMAGE PROCESSING SYSTEM	2
1.5	RESEARCH OBJECTIVES	3
2.0	**SYNTHETIC APERTURE RADAR IMAGERY**	4
2.1	FORMAT	4
2.2	IMAGE SETS	4
2.3	CHARACTERISTICS	5
2.4	GROUND TRUTH	7
3.0	**RADON TRANSFORM**	10
3.1	DEFINITION	10
3.2	IMPLEMENTATION	14
4.0	**TRANSFORM EVALUATION**	15
4.1	DEFINITIONS	15
4.2	AUTOMATIC DETECTION ALGORITHM (ADA)	16
4.3	GROUND TRUTH COMPARISON	17
5.0	**PRELIMINARY TESTING**	18
5.1	BASIC TEST	18
5.2	CLIPPED TRANSFORM	18
5.3	MANUAL SHIP REMOVAL	18
5.4	SEMBLANCE STUDIES	18
5.5	PRELIMINARY RESULTS	19
6.0	**IMAGE AND TRANSFORM SIZES**	21
6.1	THEORY	21
	6.1.1 Input Image	21
	6.1.2 Radon Transform	22
	6.1.3 System Optimization	23
	6.1.3.1 Optimal Image Size	23
	6.1.3.2 Optimal Transform Size	24
6.2	SIZE OPTIMIZATION EXPERIMENTS	24
	6.2.1 Test Sets	24
	6.2.2 Processing	24
	6.2.3 Results	25
7.0	**STANDARD IMAGE SETS**	30

TABLE OF CONTENTS (cont'd)

		Page
8.0	**BASELINE ALGORITHM**	31
8.1	DESCRIPTION	31
8.2	TRANSFORM CHARACTERISTICS	31
	8.2.1 Effect on Image Features	31
	8.2.2 Grey Level Statistics	32
	8.2.2.1 Ocean Transform Statistics	32
	8.2.2.2 Ship Image Statistics	34
	8.2.2.3 Results	40
8.3	ADA PERFORMANCE	40
8.4	COMPARISON OF ADA TO VISUAL EXAMINATION	42
	8.4.1 Procedure	42
	8.4.2 Results	42
8.5	ADDITIONAL TESTING	44
9.0	**NORMALIZED EMPTY OCEAN ADA**	46
9.1	EMPTY OCEAN CHARACTERIZATION	46
9.2	NORMALIZATION METHOD	47
9.3	RESULTS	48
10.0	**PEAK SHAPE MEASUREMENT**	51
10.1	LOCAL SIGMA	51
	10.1.1 Results	51
10.2	BOWTIE SHAPE RECOGNITION	53
	10.2.1 Algorithms	53
	10.2.1.1 Bowtie_1	53
	10.2.1.2 Bowtie_2	53
	10.2.2 Results	55
11.0	**SEMBLANCE**	58
11.1	SEMBLANCE FILTER PREPROCESSOR	59
	11.1.1 Algorithm Implementation	59
	11.1.2 Results	59
11.2	SLANT STACK TRANSFORM	60
11.3	DIRECTIONAL SEMBLANCE PROCESSING	61
	11.3.1 Definition	61
	11.3.2 Initial Testing	61
	11.3.3 DSF System Implementation	62
	11.3.3.1 Processing Details	63
	11.3.3.2 Filter Definition	64
	11.3.4 Preliminary Investigation	66
	11.3.4.1 Transform Combination Methods	66
	11.3.4.2 Comparison Between Filtered and Unfiltered Images	67
	11.3.5 Detailed Evaluation of Selected Filters	67
	11.3.6 Results	69
11.4	NORMALIZED DIRECTION SEMBLANCE	69
	11.4.1 Results	69
11.5	SEMBLANCE AND PEAK SHAPE	73
12.0	**CONCLUSIONS**	75
13.0	**RECOMMENDATIONS**	77

TABLE OF CONTENTS (cont'd)

Page

APPENDIX A IMAGE SETS

APPENDIX B RADON TRANSFORM ALGORITHM

APPENDIX C IMAGES

ABSTRACT

A system to automatically detect ship wakes in synthetic aperture radar ocean images has been developed. The basic system does the Radon transform of the SAR image, then detects bright and dark peaks produced in the transform by wakes in the image. It was tested on a set of 26 400x400 Seasat images; it had a probability of detection (PD) of 0.46 for individual wake components, and a false alarm rate (FAR) of 9 alarms per 512x512 area. It detected at least one wake component for every ship in the images.

A number of additional processing techniques were developed and tested, including normalizing the Radon transform to image line length, automatically analyzing the shape of the peaks in the transform, and applying various semblance filters to the image. The most successful were the shape detection and directional semblance. Shape detection reduced FAR to 0.5, without affecting PD. The directional semblance increased dark wake peak heights by up to 50%, and increased PD from .23 to .31 for dark wake components.

SUMMARY

0.1 INTRODUCTION

This report describes research done on the use of the Radon transform to automatically detect ship wakes in synthetic aperture radar (SAR) images of the ocean. The research objective was to implement the Radon transform, apply it to a number of actual images of ship wakes, and evaluate its usefulness for wake detection. It was also intended to study other processing techniques that might be useful, and to collect information on the characteristics of SAR ship wakes images.

0.1.1 SYNTHETIC APERTURE RADAR IMAGES

SAR is an active microwave imaging system. The images resemble visible photographic images, but have considerable speckle noise.

The SAR data were provided as complex images, these were converted to real images by taking the magnitude of the complex numbers and compressing the images to 8 bits. The images were manually ground truthed, by examining them and outlining visible wake components.

0.1.2 THE RADON TRANSFORM

This transform integrates the image intensity along every straight line through the image; each integral becomes a single element in the transform. Any line which is brighter or darker on average than its neighboring lines will produce a transform element which is brighter or darker. Thus a bright line will create a bright spot in the transform, even if the line is noisy or broken.

The lines in the image were represented in polar coordinates by the length and angle to the x-axis of the perpendicular from the line to the origin. The length, ρ, could be positive or negative; the angle, θ, varied from 0 to 180 degrees.

The transform consisted of a rectangular array. The column index of an element gave the θ value for the associated line, the row index gave ρ.

0.1.3 AUTOMATIC DETECTION ALGORITHM (ADA)

An algorithm was implemented to examine the Radon transform for peaks and compare the lines represented by the peaks with the ground truth, to determine the effectiveness of the transform. The process determined bright and dark thresholds from the statistics of the transform, then found the extreme points in each area of the transform which exceeded these thresholds. These points were converted back to lines and compared with the ground truth to measure performance. This was specified in terms of:

1. Wake Probability of Detection (PD) - The ratio of the number of wake components detected in a set of images to the total number in the images.

2. Ship Probability of Detection (Envelope PD) - The probability that at least one wake component from a ship is detected.

3. Wake False Alarm Rate (FAR) - The average number of false alarms in a 512x512 image.

0.1.4 COMPUTER SYSTEM

Two systems were used in the research. An IBM AT based IMAVISION system was used for image display and some processing; a VAX 11-750 was used for the transforms and other intensive processing.

0.2.0 PRELIMINARY TESTING

The following preliminary tests were done on a set of 12 images, of varying sizes.

1. The basic transform and ADA were applied to the original images.

2. Pixels in the images due to bright ships were removed from the images, the transform and ADA were then applied.

3. The entire ship was manually removed from each image, leaving only the wake, before the transform was applied.

4. A 3x3 semblance filter was applied to the images before the transform was done. This filter is discussed in more detail below.

5. Sets of 400x400 and 256x256 images were windowed from the images, and 512x512 and 256x256 transforms applied to them, to determine optimum sizes for further testing.

The preliminary tests showed the following:

1. PD was typically 0.5 for bright wakes, and 0.2 for dark wakes, for all the methods tested.

2. FAR was typically 15 for bright wakes and 5 for dark wakes.

3. The probability of detecting at least one component of a ship's wake was 1 for almost all methods tested.

4. Performance was improved by removing the ship, manually or by clipping bright pixels.

5. A 400x400 image size might be slightly better than the 256x256 size. The results showed no preference for the transform sizes tested.

0.3.0 DETAILED TESTING

A standard set of 26 400x400 images was used for most of the remaining testing. It consisted of 26 images; 12 showed empty ocean, 8 contained only wakes, and 6 contained both ship reflections and the associated wake components.

The test results are summarized in Table 0.2, which gives PD, envelope PD, and FAR for each process. Note that FAR was determined from ocean background images, and hence is the same for images containing ships and wakes and images containing only wakes.

3.1 BASELINE TESTS

The baseline Radon transform was applied to the standard set; the results are summarized in the table. The transforms were examined to see if the ADA was limited by the existence of peaks due to the wake components. It was found that essentially all wake components produced peaks in the transform; generally the ADA did not detect some because they were below its threshold.

The statistics of the transforms were also examined. The transform grey levels did not have a Gaussian distribution; the centre was higher and the tails

TABLE 0.1

PERFORMANCE SUMMARY

Images containing ships and wakes

6 images, 13 wake components

Algorithm	Bright Wakes PD	Bright Wakes FAR	Dark Wakes PD	Dark Wakes FAR	Envelope PD
Baseline	.46	6.3	.23	2.7	1.0
Normalized and using empty ocean statistics	.31	11.7	.31	5.1	.83
Using variance around peak	.46	1.2	.23	0.3	1.0
Bowtie	.46	0.2	.23	0.3	1.0
Semblance D	.53	7.8	.31	8.9	1.0
Semblance E	.53	4.5	.31	7.5	1.0
Semblance D normalized and using adjacent ocean statistics	.38	10	.31	11	.83
Semblance E normalized and using adjacent ocean statistics	.54	7.0	.23	1.6	.83
Semblance E and bowtie	.53	0.4	.31	0.2	1.0

TABLE 0.1 (cont'd)

PERFORMANCE SUMMARY

Images containing wakes only

8 images, 17 wake components

Algorithm	Bright Wakes PD	Bright Wakes FAR	Dark Wakes PD	Dark Wakes FAR	Envelope PD
Baseline	.47	6.3	.24	2.7	1.0
Normalized and using empty ocean statistics	.65	11.7	.18	5.1	1.0
Using sigma around peak	.47	1.2	.24	0.3	1.0
Bowtie	.41	0.2	.18	0.3	1.0
Semblance D	.65	7.8	.18	8.9	1.0
Semblance E	.59	4.5	.18	7.5	.88
Semblance D normalized and using adjacent ocean statistics	.35	10	.18	11	.88
Semblance E normalized and using adjacent ocean statistics	.41	7.0	.23	1.6	.88
Semblance E and bowtie	.47	0.4	.17	0.2	1.0

were wider than expected for a Gaussian. When the statistics of transform elements representing a uniform line length in the original image were studied they were found to be Gaussian. The standard deviation varied approximately as the square root of the line length for lines up to about 300 pixels long, beyond that the variation became erratic.

0.3.2 NORMALIZATION TESTS

The dependence of the grey level distribution of the transforms on the line length suggested normalizing the transform to this length, to correct the peak heights, so the detection sensitivity of the ADA would be uniform over the entire transform.

In the same tests the ADA threshold was obtained from an empty ocean region adjacent to the region being searched, so that the ADA threshold was not affected by the presence of a ship or wake in the image.

The results of the normalization tests are given in the table. They indicate that PD is similar to the baseline tests, but FAR seems to be increased. The increase was due to two images which were not well matched with the background images. If the anomalous images were removed from the data set the false alarm rate was considerably lower than the baseline ADA.

0.3.3 SHAPE MEASUREMENT

Examination of the Radon transforms indicated that peaks due to wakes tended to have a 'bowtie' shape, with two bright arms, while false alarm peaks tended to be more uniform. Two shape detection algorithms were developed and tested to see if they could be used to reduce FAR.

The first algorithm simply measured the variance of the transform grey levels around the peak; it was expected that a peak due to a wake would have a greater variance than a false alarm peak. A second more powerful algorithm, the bowtie algorithm, was developed to actually measure the bowtie shape around the peak. The results of these procedures are shown in the table. The test results indicate that such shape detection algorithms are very useful in reducing FAR.

0.3.4 SEMBLANCE

Semblance is a second order statistic measuring the amount of variation in a set of data. It is defined as the square of the mean of the data divided by the mean of the squares of the data. The semblance is normalized to a range of between 0 and 1. A semblance of 1 indicates no variation, a semblance close to 0 represents maximum variation.

Previous research had suggested that the semblance might be useful in distinguishing wakes from background ocean. This project tested several methods of using the semblance.

1. The image was filtered by determining the semblance over a 3x3 window applied to each image pixel. The resulting semblance image was multiplied by the original image. The Radon transform and ADA were applied to this product. This semblance filter had little effect on the system performance, and no further development was done.

2. The Radon transform was modified so that instead of measuring the sum of the pixels along each line it measured the semblance of the pixels along the line. This is known as the slant stack algorithm. The transform was applied to the standard image set, the results were not promising. Wake peaks were less visible than in the baseline transforms. No further work was done on the slant stack.

3. A directional semblance filter was implemented. This found the semblance along lines 15-20 pixels long in 4 directions (\/|-) through each pixel. Thus it produced four directional output images. The images were transformed, and then the transforms were combined by taking the area from each transform corresponding to the closest filter direction. Two filters were evaluated in detail, filters D and E. The results are given in the table, they indicate a generally increased PD. FAR is also increased for dark wakes, because the procedure enhances all dark lines.

The line length normalization and peak shape false alarm reduction methods were applied to these semblance filtered transforms. The normalization had little obvious effect, the shape measurements reduced FAR.

0.4.0 CONCLUSIONS

1. A Radon Transform combined with a simple automatic peak detection algorithm can automatically detect almost all visually obvious wake components in a SAR ocean image, with a false alarm rate of much less than one false alarm per 512x512 image.

2. The detection performance for the various combinations of processing do not show great differences, partly due to the small number of images used for testing.

3. Bright ship and other non ocean features such as shorelines are a hindrance to wake detection, and if possible they should be removed from the image before looking for wakes.

4. The detection algorithm should take into account the variation in length between lines associated with different elements in the transforms.

5. Using statistics from empty ocean regions to adjust the peak detection algorithm parameters appears to be useful, but may be difficult to do automatically.

6. Algorithms which examine the peak shape in the transform, such as the bowtie filter, are able to differentiate wake peaks from false alarms quite reliably.

7. The directional semblance filter enhanced dark wakes, and in most cases improved system performance on both bright and dark wakes. The peak shape and line length normalization technique can be applied to these algorithms as well.

1.0 INTRODUCTION

Synthetic aperture radar can produce detailed ground images from satellites or aircraft, through almost any weather conditions and with no dependence on external illumination, and is therefore very useful for surveillance or remote sensing (Colwell, 1983). It has been found that some ship wakes appear very distinctly in SAR images, as straight lines readily visible on the ocean background (Wilmut, 1986). This report describes research to investigate the use of the Radon transform in the automatic image analysis system for detection of these wakes.

1.1 SHIP WAKES

A moving ship produces a set of waves on the water forming a characteristic wake pattern behind it. The hydrodynamics of wake formation is well understood, and is similar for most displacement vessels. The wake occupies a V shaped region behind the ship, and can be visible over a length of several kilometres. The arms of the V have a maximum angle of about 19 degrees from the centre line. The wakes seen in SAR images can generally be divided into four components: the Kelvin wake, the turbulent wake, the narrow-V wake and internal waves (Tunaley, ?; Case, 1984; Hammond, 1985). The Kelvin wake is the regular arms of the V, at an angle of 19 degrees from the centre. The turbulent wake is the central wake, directly behind the ship. The narrow-V wake appears as a V which has a smaller angle than 19 degrees. Internal waves are waves which are set up beneath the water surface, but intersect the surface and affect its appearance.

Detection of the ship wake may be useful for two reasons. The wake may be more visible than the ship, and thus it may be useful to detect the ship from its wake. The wake also may provide information on the course, speed, or characteristics of the ship.

1.2 SYNTHETIC APERTURE RADAR

SAR is a microwave imaging system similar to a standard radar (Colwell, 1983). The difference is that the SAR antenna is moved linearly, in a satellite or aircraft, and the range of the target is determined by using both return time and Doppler shift. This allows synthesizing of an effective

antenna size which is much larger than the actual antenna size, and hence gives very high resolution images. The disadvantage of SAR is that it requires intensive computation to convert the returned signal to an image, and the image contains speckle noise due to the coherent nature of the imaging mechanism.

The exact mechanism by which ship wakes and other waves are imaged by SAR is not well understood. Bragg scattering, in which reflections are produced by surface waves with wavelength matching the radar wavelength, is thought to explain most ocean scatter phenomena. Waves of much longer wavelength than that of the radar are visible in SAR images. It is thought that the larger waves may influence the shape of the shorter waves which the Bragg mechanism images. For example the turbulence behind the ship may dampen capillary and small surface gravity waves, decreasing the Bragg scattering and making the region appear dark in the SAR image.

1.3 RADON TRANSFORM

The Radon transform integrates image intensity along straight lines crossing the image. It was therefore expected to improve the signal to noise ratio for straight line features in an image, since intensity noise in such features would be averaged out in the transform. The transform was also suited to the noisy, discontinuous nature of SAR wake images, since it did not depend on a line being connected or continuous for detection (Wilmut, 1986). Furthermore the output, which concentrates all of the information for a given line in one transform element is very suited for automatic detection and analysis methods.

Previous research showed that the transform did improve the signal to noise ratio to ocean images. Some promising preliminary work had been done on wake enhancement using the transform, and it was felt that it should be extended, using actual SAR wake data.

1.4 IMAGE PROCESSING SYSTEM

Two computer systems were used in doing this research, an IBM PC/AT based IMAVISION and a VAX 11-750.

The IMAVISION system was an RBA proprietary image analysis and display system running EASI/PACE image analysis software. It could display a 3 colour

512x512 image and up to eight graphics planes, and was designed for remote sensing and image analysis tasks. The IMAVISION was used for displaying the images and transforms, and measuring their characteristics. It was also used for some of the image processing such as the directional semblance filtering. It was connected to the VAX by a high speed parallel data link, so that images could be transferred rapidly between the systems.

The VAX also ran the EASI/PACE image analysis system, but had no display facility. It was used for memory intensive processing applications, such as doing the actual Radon transforms. It was also used for image storage and backup, and for reading images supplied on tape.

1.5 RESEARCH OBJECTIVES

The main objective of the research was to implement the Radon transform, apply it to a number of actual SAR shipwake images, and evaluate its usefulness in a wake detection system. The research was also designed to collect information on the properties of SAR wake images, to study other image processing techniques which might improve wake detection, and to investigate the addition of coherency techniques or other modifications to the Radon transform.

2.0 SYNTHETIC APERTURE RADAR IMAGERY

The images used in this study were obtained from Seasat data. The wake regions were initially identified by CRC from optically processed data. These regions were then reprocessed digitally, and the resulting images provided to RBA. This section describes the processing, characteristics, and ground truthing of these data.

2.1 FORMAT

The digital images were arrays of complex numbers, with each complex number representing a single pixel in the image, and consisting of two 32 bit real numbers. The data was written in excess 64 notation, in Perkin-Elmer format. A program was written to convert the data to VAX format, find the magnitude of each pixel, linearly compress the data into 8 bits, and store the resulting 8-bit compressed image in the UNIDSK format used by the IMAVISION system.

Initially the compression was determined by examining the histogram of the 32 bit magnitude image, and choosing the limits to contain essentially the entire range of pixel values. It was found that the range of the data between images was generally quite consistent, so to minimize the variables in the system the fixed range of 0.5×10^{-4} to 0.75×10^{-2} was used for all images.

2.2 IMAGE SETS

Four sets of SAR images were used for this research; preliminary images, the size optimization set, the standard image set, and the additional image set. These sets are described in detail in Appendix A.

The preliminary image set consisted of 7 images containing wakes, and 5 images containing only ocean background. It included images with sizes ranging from 256x256 to 400x1344.

The size optimization set consisted of 7 400x400 wake images and 3 400x400 ocean images. A 256x256 image was windowed from each of these.

Research on the size optimization set indicated that a standard image size of 400x400 should be used. A set of this size, the standard image set, was extracted and used for most of the detailed testing. It consisted of 26 images, 12 showing empty ocean, 8 containing wake only, and 6 containing both a ship and its associated wake.

Some additional ship and sea images were analyzed later in the project. The set consisted of 16 400x400 images. Of these, 11 contained ships and wakes, and 5 were images of ocean background.

2.3 CHARACTERISTICS

The Seasat data were processed to produce images with square pixels, 25 metres on a side. The ocean grey levels within each image have a Rayleigh distribution, as can be seen in Figure 2-1.

The images showed very few details over most of the ocean area. Some of the images did show ocean features such as lines or areas with different brightness; these were probably caused by variations in the ocean surface due to wind, current, or internal waves. As well there were parallel striations in one image, probably showing ocean waves of length comparable to or larger than the 25 metre resolution of the radar.

The images also contained SAR speckle noise. This noise is typical of coherent imaging systems, and is due to constructive or destructive interference between returning signals from different regions within a given pixel. The noise is multiplicative and can not be easily eliminated by standard noise reduction techniques.

The images were not isotropic; they usually appeared to have short linear features running horizontally across them. These were probably due to the functioning of the SAR system, which uses different methods to resolve features in the cross-track and along-track directions. No research was done on this anisotropy, and it was not taken into account when calculating performance.

A ship generally appeared in the images as a bright area, with one or more visible wake components associated with it. The SAR system uses the Doppler shift of the return signal in determining the position of the target, the velocity of the ship can alter this shift and therefore cause the ship to be displaced in the image. For this reason the wakes did not always appear to start at the ship, the exact offset depended on the speed and direction of the ship's travel. Some images showed definite wakes with no obvious associated ship image.

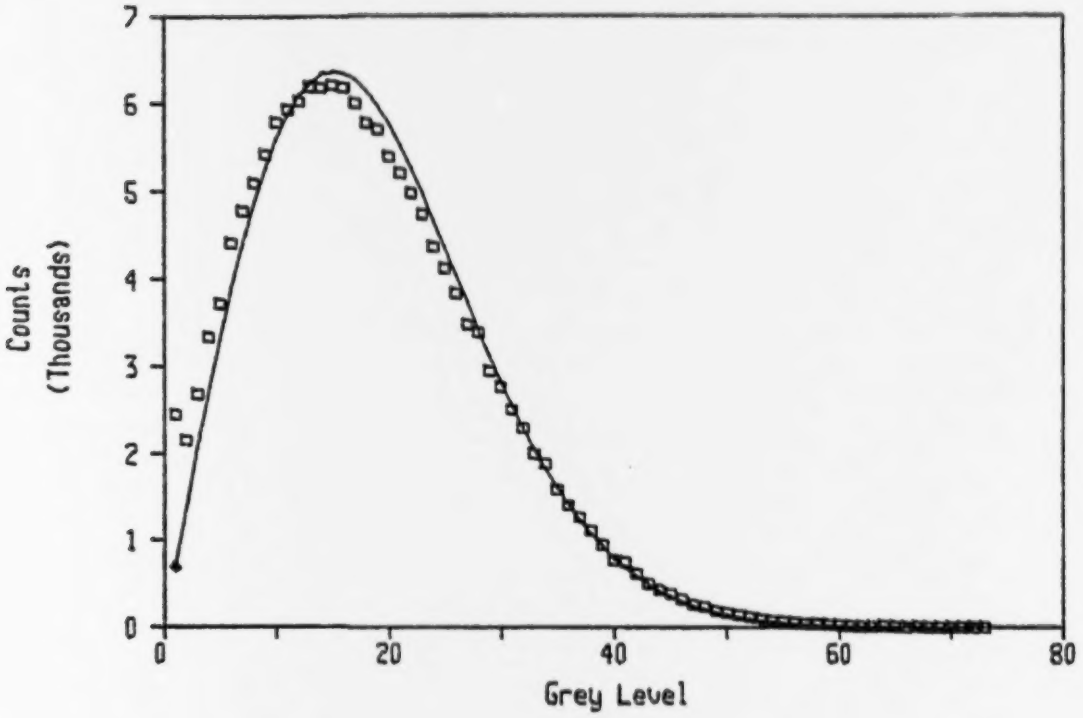

FIGURE 2-1

Grey level distribution for Seasat ocean images.

The squares show the histogram of the grey levels of the 400x400 Seasat ocean image 9-s-1. The line is a Rayleigh distribution fit to the data.

The wakes appeared as bright or dark lines, generally in a V-shape, and converging at the ship. It was difficult to classify the wake components exactly; in general there were two basic types:

1. Turbulent wakes - the wake area directly behind the ship, generally a dark line.

2. V-Wakes - the Kelvin arms, at an angle of up to 19 degrees on either side of the turbulent wake.

These were not always all visible, and components could be seen at all angles from the centre up to the 19.5 degree maximum.

2.4 GROUND TRUTH

Ground truth is ideally an independent determination of the characteristics or features of the region being studied by the remote sensing system; it can be obtained, for example, by using data from a ground survey or from a different type of remote sensing system. The important characteristic is that it provides an independent check of the methods being tested.

Unfortunately there are no independent data available on the presence of ships or the wake characteristics of these ships for the Seasat data. The ground truthing was instead done from visual examination of the Seasat images themselves. Each ocean area containing a separable visible part of a wake was outlined and considered as a single wake component. An example of such outlines, and a definition of the base, sides, and top, are given in Figure 2-2. Such a component could consist of a long thin straight line, for example with a base and top each 5 pixels, and a side of 100 pixels, or an extended area, for example a rhombus with a top of 5 pixels, a side of 100 pixels, and a base of 50 pixels. The only requirement was that the area outlined be entirely filled with a distinguishable wake region, with uniform appearance, that could not be visually split up into two or more smaller regions. For a detected line to be a part of the wake it had to pass through the base and the top of one of these components.

A component could contain a region brighter than the ocean background, a region darker than the background, or both. It was often impossible to define a component as a "bright wake" or a "dark wake", since many contained both bright and dark

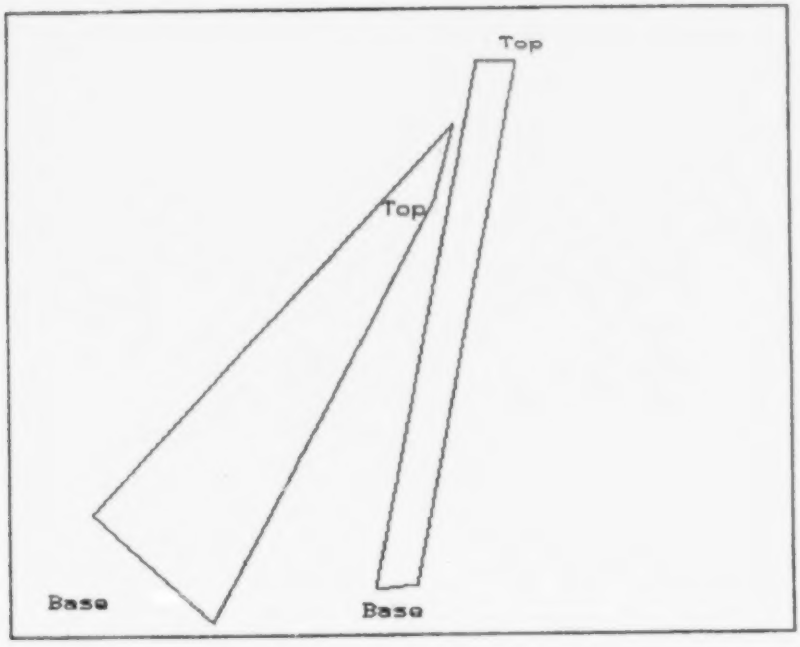

FIGURE 2-2

Ground truth for image 9-v-1.

The outlined areas indicate distinct wake components. A detected line was considered a match to a component if it passed through the base and top of the component.

regions. When human observers see and ground truth a distinct wake region they may be seeing an area which is brighter or darker than the background, or they may be seeing an area with a different texture but which has the same average level as the background.

The presence of ships had an effect on the ground truthing. In many of the images the bright ship images were very obvious. In others the ships were not visible, but one or more obvious wake components could be seen. In either case marginally visible wake components would be identified as wakes, whereas if the same component had not been close to an obvious ship or wake it would have been ignored.

3.0 RADON TRANSFORM

The Radon transform measures straight line features in an image (Rosenfeld, 1982). It works by integrating the image intensity along a straight line crossing the image; this sum becomes a single element in the transform. This process is repeated for every possible straight line in the image; any such line is thus represented by a single element in the transform.

If the pixels along the line in the original image are, on average, of different intensity than the surrounding pixels, then the corresponding transform element should have a value different from its surrounding elements. Therefore, for example, a bright straight line will appear as a bright spot in the transform. This is true even if the line is broken or noisy.

3.1 DEFINITION

The Radon transform is defined for a continuous image by:

$$f(\rho,\theta) = \int_D g(x,y)\ \delta\ (\rho - x\cos\theta - y\sin\theta)\ dxdy$$

where D is the entire image plane (Deans, 1981; Duda, 1972).

$g(x,y)$ is the grey level at position (x,y).

δ is the Dirac delta function.

ρ is the radius coordinate of a straight line, as defined in Figure 3-1.

θ is the angle coordinate of a straight line, as defined in Figure 3-1.

$f,(\rho,\theta)$ is the radon transform of g.

Thus $f(\rho,\theta)$ is the integral of the image grey levels along the line defined by ρ and θ as indicated in Figure 3-1. If the Radon transform is displayed as an image in the (ρ,θ) plane, then a bright or dark spot in the transform image corresponds to a bright or dark line in the input image. The (ρ,θ) coordinates of the line are given by the position of the spot. The transform does not rely on the line being connected to detect it, even a broken or noisy line can still produce a spot in the transform. The only requirement is that the sum of the pixel grey levels along the line is different from the sum along nearby lines.

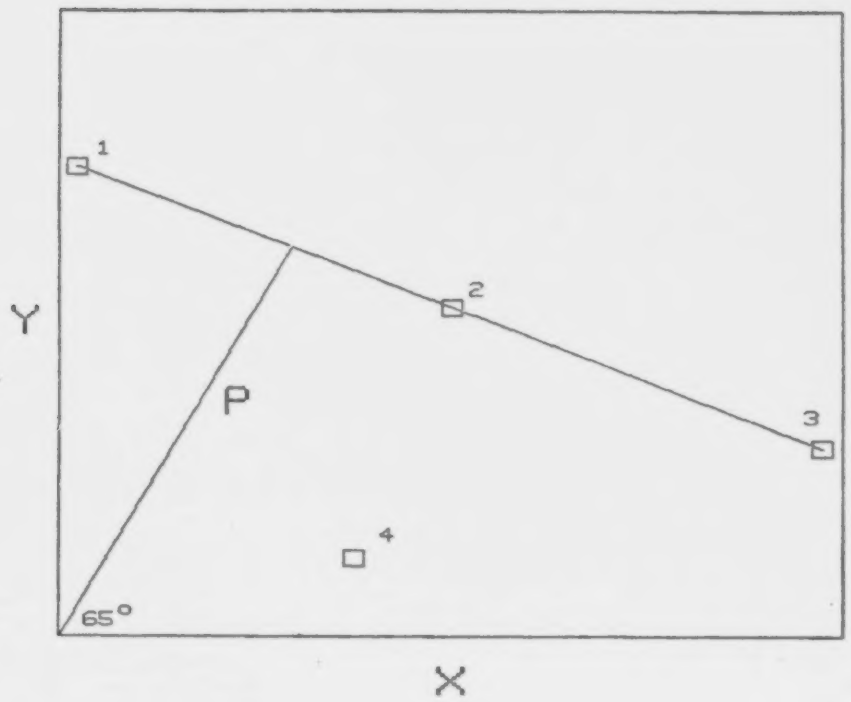

FIGURE 3-1

Image containing four points. Points 1, 2, and 3, form a straight line. Any such straight line in the image can be described in terms of its radial coordinates. A perpendicular is drawn from the line to the origin. Then the line is specified by ρ, the length of the perpendicular, and θ, the angle the perpendicular makes with the x-axis. For the line shown $\rho = 275$, $\theta = 65$ degrees. This coordinate system is used in doing the Radon transform.

A line can have multiple coordinates in this system; for example the line shown also can be defined by $\rho = 275$, $\theta = 245$. For this research the limits were taken with $0 < \theta < 180$, preventing such multiple definitions.

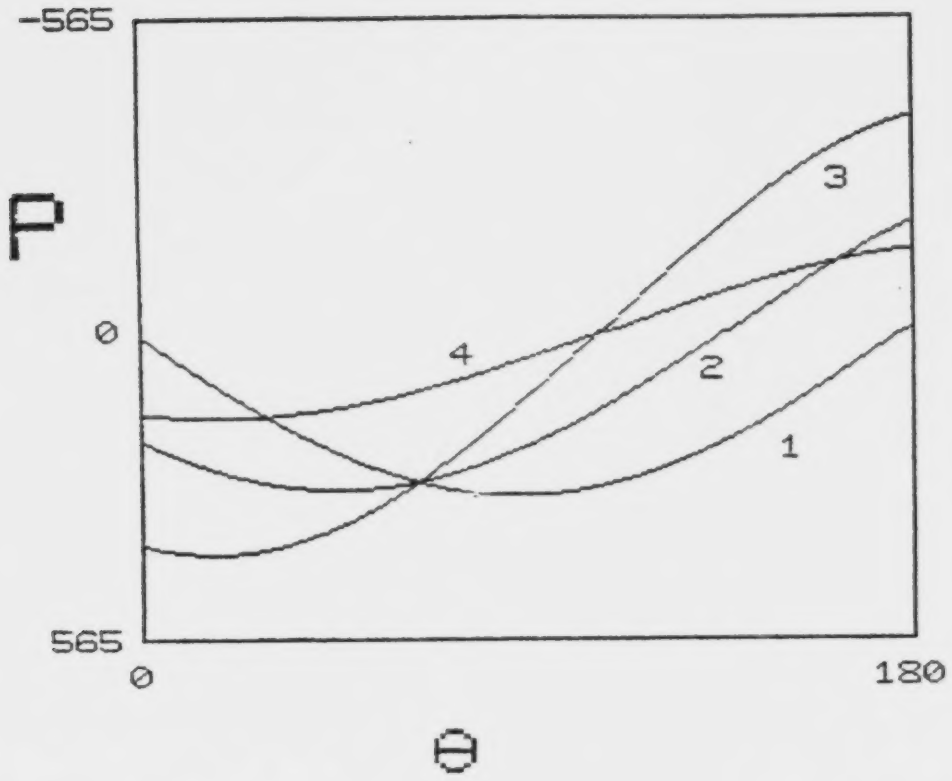

FIGURE 3-2

The Radon transform of Figure 3-1. Each point in figure 3-1 produces a sinusoidal line in the transform. The lines from points 1, 2, and 3 cross at the point $\rho = 275$, $\theta = 65$. In an actual transform the lines would add at this point, producing a dark or light spot.

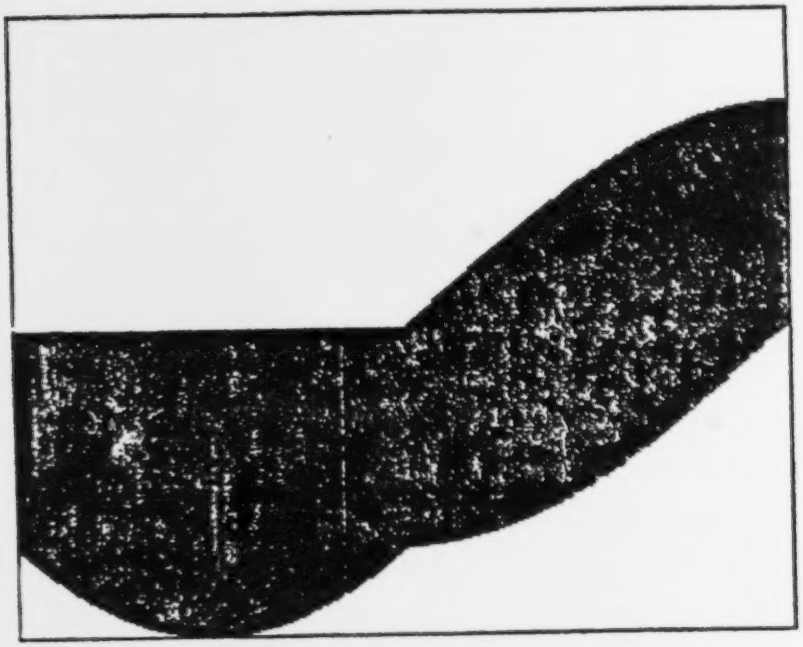

FIGURE 3-3

The dark area is the area in the Radon transform that corresponds to lines actually falling within the image, for a 400x400 image. Lines defined by the elements in the light area do not cross the image.

3.2 IMPLEMENTATION

For this study the transform was implemented in the spatial domain, using the algorithm described in Appendix B (Murphy, 1986). This method begins by creating a zeroed Radon transform array. The image is then scanned pixel by pixel, and each pixel value is added to the cells along the appropriate sinusoidal curve in the transform. The implementation allows a constant to be subtracted from the image pixel values before doing the transform. Generally this constant was set to the average image grey level (the image mean). The number of pixels added into each transform element varies; if the image mean is not subtracted this variation increases the range of the transform, and thus reduces the resolution. The output elements are calculated exactly, but are then scaled to a range of 0-255. The original range of the transform is stored so that it is available if required.

The output Radon transform format consists of a rectangular array of size up to 512x512; the axes are defined in Figure 3-2. The transform is connected across its sides since, for example, a line with θ=0 degrees and radius +R is equivalent to a line with θ=180 degrees and radius -R. Therefore any a element in the rightmost column of the transform is logically adjacent to an element in the leftmost column. Figure 3-3 shows part of the rectangular transform that actually corresponds to lines within the image, since some points on the transform represent lines which do not pass through the image at all.

The transform was implemented on the VAX computer. Most of the algorithm was written in Fortran. The inner loop, which sums each image pixel into the transform elements, was written in assembler for increased speed.

4.0 TRANSFORM EVALUATION

Algorithms were implemented to search the output Radon transforms for bright or dark peaks, and to compare the lines defined by these peaks with wakes in the original image. These algorithms are described in this section.

This procedure was necessary to provide an unbiased measure of the effectiveness of different algorithms. The system was also designed to speed up the evaluation of a process, by automating much of the analysis of the output transform.

The evaluation system was designed as simple procedures to compare relative performance of the transform and their associated processing. It was not designed to be a highly effective operational wake detector. Therefore the absolute performance is much less meaningful than the relative performance. The overall performance of the algorithm indicates only what can be easily done with a simple detection algorithm, and represents at best a lower bound on optimal system performance.

4.1 DEFINITIONS

A number of specific terms are used in this section,, and throughout the remainder of the report. They are defined here.

1. Wake Component - A single uniform, distinguishable area in the image, produced by the passage of a ship.

2. Wake - All of the wake components in an image which have been produced by a single ship.

3. Bright Wake - A wake component detected as a bright line by the automatic detection algorithm.

4. Dark Wake - A wake component detected as a dark line by the automatic detection algorithm.

5. Wake Probability of Detection (PD) - The ratio of the number of wake components detected to the number in the image. This can be given for bright wakes, dark wakes, or both. Note that wake components are not defined as bright or dark, and can be detected as either or both.

6. Envelope Probability of Detection (Envelope PD) - The probability that at least one wake component from a ship is detected.

7. Wake False Alarm Rate (FAR) - The average number of incorrect wake components detected in a 512x512 image. This can be given for bright wakes or dark wakes.

8. Image FAR - The sum of the bright wake FAR and the dark wake FAR.

4.2 AUTOMATIC DETECTION ALGORITHM (ADA)

The ADA was developed to provide an independent method of detecting peaks in the Radon transform. The algorithm works as follows:

1. The mean, m, and standard deviation, σ, of the transform are determined. These statistics are determined only from the elements corresponding to lines that lie within the original image.

2. A threshold is taken as $m \pm (K * \sigma)$, depending on whether bright or dark peaks are being located. K is a user defined parameter, and was usually chosen K=4.

3. The image is thresholded to produce a bitmap of the bright or dark regions.

4. The bitmap is dilated once, to join regions which are separated by only one or two pixels. Dilation is done by adding to the bitmap all non-black pixels which have one or more black neighbors.

5. The bitmap is labelled, uniquely identifying each connected region. Two elements are connected if they are horizontal, vertical, or diagonal neighbors; a region is connected if any two elements in it can be joined by a chain of connected elements which are in the region.

6. The peak element of the original transform in each labelled area is found. These peaks correspond to the strong lines in the original image.

7. Regions in the bitmap which are logically adjacent across the edges of the transform are identified by comparing the labels of the two edges. The brightest or darkest of equivalent peaks is taken as the actual peak.

8. In some cases the detected peaks were thresholded again at values of Nσ, with N=4.5, 5.0, ... This determined how raising the threshold would change the performance of the system. Because this second thresholding was done after the peaks had been detected it did not provide the same results as would have been obtained from setting K to a different value in step 2. However the results are similar, and the procedure used is much faster and simpler to interpret.

4.3 GROUND TRUTH COMPARISON

A semi-automatic algorithm was developed to compare the results of the ADA with the ground truth. The algorithm read the output of the ADA, and plotted the detected lines on the IMAVISION display, overlaid on a display of the original image ground truth. The user could then indicate if the line detected was a correct detection or a false alarm. The final results were tabulated automatically.

5.0 PRELIMINARY TESTING

Initial development and testing of the Radon transform and automatic detection algorithms was done on a set of 12 images. These are listed in Appendix A. The sizes ranged from 256x256 to 400x1344. The following preliminary studies were done using these data, to characterize system performance and determine subjects for more detailed studies.

5.1 BASIC TEST

The Radon transform and ADA were applied to the images. The value k=4 was used in the ADA. This value was determined experimentally, to provide reasonable system performance.

5.2 CLIPPED TRANSFORM

The ship reflections often appear as a few very bright pixels in the images. These bright spots cause bright lines in the transform which can conceal peaks due to wakes or cause false alarms. The transform was modified so that any pixel brighter than a user specified clipping level would be replaced by the average pixel brightness, effectively removing its contribution to the transform. It was found that a clipping level of 160 effectively removed the bright ship reflections without affecting wakes or ocean pixels. This clipping was incorporated into the transform, and the performance measured.

5.3 MANUAL SHIP REMOVAL

The clipping algorithm removed very bright ship reflections, but left less bright parts of the ship still in the image. To see if further ship removal might improve the system the images were manually altered to replace the entire ship region by the average grey level.

5.4 SEMBLANCE STUDIES

Semblance is a statistical measure of the variation of a signal (Stoffa, 1981). It was thought possible that it could be used as a wake enhancement filter, so some semblance measurements were done on the preliminary image set. These measurements and results are tabulated here, but are discussed in detail in Section 11.

5.5 PRELIMINARY RESULTS

The results of the preliminary measurements are given in Table 5-1.

The results indicate that removing the ship improves performance. The decrease in the clipped PD compared to the basic PD is due to the basic algorithm detecting the bright ship pixels rather than the wake. In the other cases removing the ship gives the same or lower FAR and an improved PD. The semblance filter tested here did not appear useful in enhancing the wakes, or improving the ADA performance.

The preliminary testing also indicated that a standard image size should be used for further testing. The varying image sizes used in the preliminary set introduced additional variables into the system, requiring additional effort to process the images and interpret the results. Furthermore it was apparent that the images had been chosen to contain a complete wake with little background ocean; thus the image size indicated the shape and presence of a wake, introducing a bias into the measurements.

TABLE 5-1 PRELIMINARY RESULTS

	Bright Wakes PD	Bright Wakes FAR	Dark Wakes PD	Dark Wakes FAR	Envelope PD
Basic System	0.53	16.1	0.18	3.5	0.87
Clipped	0.47	12.2	0.18	4.8	0.87
Ship Removed	0.59	17.5	0.18	4.6	0.87
3x3 Semblance	0.47	11.1	0.12	6.1	0.87

6.0 IMAGE AND TRANSFORM SIZES

A study to determine appropriate sizes for the input image and for the Radon transform bins is described in this section. This includes both a brief theoretical discussion of the optimal sizes and some experimental measurements of detection efficiency as a function of size.

6.1 THEORY

6.1.1 Input Image

The Radon transform can be applied to an image of any size or shape; it is not limited to square or rectangular images. In this section factors affecting the size and shape are discussed.

The time taken to compute the transform is approximately proportional to the area of the image. In practical application the area is effectively fixed by the ocean area which must be searched for wakes. Therefore the image size for each transform should not affect the overall computing time; the system can either do many fast transforms on small windows or fewer slower transforms on large windows. The total time will be approximately the same. Furthermore, if the same coordinate system is used, the Radon transforms of adjacent areas can be added element by element to produce the transform of the total area.

Further processing steps, such as the peak detection algorithm, may depend on image size. These processes will probably require small amounts of time compared to the Radon transform itself, so should not affect the overall computing load.

The optimal image size will depend on the expected length of the wake components. Longer components will be easier to detect than shorter ones. If the image is much larger than the length of the component, then the peak due to that component may be lost in the noise. Therefore the optimal image size is of the order of the expected length of the wake components.

The images being searched are not isotropic, they depend on a number of parameters which are directionally dependent:

1. Ship Heading
   actually appearing in the image.

2. Expected Ship Heading - The probable direction of travel of a ship being looked for.

3. Sea State - The direction the waves are travelling.

4. Platform Parameters - The SAR image is inherently directional, since different mechanisms are used to determine range in the cross-track and along-track directions.

Most of these parameters are not easily determined, particularly for the SEASAT images. The only one directly obtainable is the platform parameters. It might be worth investigating anisotropy due to these, but it was not considered in the current research.

It was therefore decided to use a square image, since this is the simplest approximately isotropic shape. A more complex shape, such as a circle, might have been useful but would have required considerable effort to implement.

6.1.2 Radon Transform

The bin size in the transform should be chosen to optimize the overall system performance. The choice may depend on factors such as SAR parameters, image quality, sea state, and expected wake parameters. It is possible to have the bin size vary over the transform; this would, for example, allow adjustment for the difference in length between a line crossing the corner of an image and one crossing the centre. In this study only a constant transform bin size was used.

The radius resolution in the transform should be chosen to match the expected wake width, so that more wake pixels will be averaged into the transform peak due to that wake. Too low resolution will, however, include non-wake pixels from the edge of the wake. To prevent this the resolution should be about half the expected wake width. A typical wake component in the images studied was 5-10 pixels wide, although this varied greatly. Thus the range resolution should be 2-4 pixels.

Once the range resolution is chosen the angular resolution can be chosen so that the lines defined by elements with identical radius values, and angle value differing by one bin will not overlap excessively.

As an example consider a 400x400 image. The range bins must cover a total range of -566 to +566 pixels. 512 radius bins would give a resolution of 2.2 pixels; 256 bins would give a resolution of 4.4 pixels. If 256 radius bins are used then the transform angular resolution should be -4/400 radians, or 0.6 degrees. This will require 300 angle bins to cover the 0-180 degree range required. Thus the transform should be approximately square, and somewhat smaller than the image.

No information is lost when bins which are smaller than the optimal size are used; it is always possible to compress the transform along one or both dimensions to get the same result as would have been obtained with larger bin sizes.

6.1.3 System Optimization

The above discussion indicates that the variables that should be optimized are related, and have a restricted range. A detailed set of experiments to optimize these parameters appeared to be unnecessary, for the following reasons:

1. The optimization would be done using an automatic detection algorithm, changes in this may change the optimal size.

2. The angle and radius bins can always be made larger after doing the transform by compressing it. Thus optimal bin size can be determined by the peak detection algorithm, provided the optimal bin size is larger than the bin size actually used.

3. The data set includes only a limited size and number of wakes.

6.1.3.1 Optimal Image Size

It was decided to test two image sizes, 400x400, and 256x256, and choose the better performing one as the standard image size. This does not preclude changing the size in the future, and in fact it is probably useful to vary the image size depending on the expected wake size and sea state.

6.1.3.2 Optimal Transform Size

The previous discussion suggested that the Radon transforms should be square, and the size should be comparable to, or slightly smaller than the image size. The transform algorithm is limited to a maximum transform size of 512x512, so it was decided to test this size and a 256x256 transform and choose the better performing one as the standard transform size.

6.2 SIZE OPTIMIZATION EXPERIMENTS

The following analyses were carried out:

1. Test sets of 400x400 and 256x256 images were chosen.
2. 512x512 and 256x256 Radon transforms were run on these images.
3. The automatic evaluation system was applied to the transforms.
4. PD and FAR were determined for various values of the threshold N.

The listed items are discussed in more detail below.

6.2.1 Test Sets

The test sets were chosen by taking appropriately sized windows from the images provided. The set chosen consisted of 7 images containing one ship and one or more wake components, 7 images containing wake components only, and 3 images containing only ocean. No images containing more than one ship were used. The 256x256 images were windows from the 400x400 images, so the same wakes were detected in each set.

6.2.2 Processing

The standard Radon transform algorithm was used. Ship peaks above grey level 160 were clipped, as the previous research indicated this might be useful. The mean grey level of the image was subtracted from each pixel grey level before doing the transform.

Five combinations of image size, transform size, and threshold were actually analyzed.

1. 400x400 Image, 512x512 Transform, Threshold=4σ
2. 400x400 Image, 256x256 Transform, Threshold=4σ
3. 256x256 Image, 512x512 Transform, Threshold=4σ
4. 256x256 Image, 256x256 Transform, Threshold=4σ
5. 256x256 Image, 256x256 Transform, Threshold=3σ

6.2.3 Results

The results of the analysis are shown in Table 6-1, and plotted in Figure 6-1, as performance curves for each set of images. It can be seen that, in general, as N is decreased PD initially rises rapidly with a slow increase in FAR, then PD saturates and FAR continues to increase. The curves allow the choice of the best value of N for the desired application.

The performance curves indicate the following points:

1. Set 12 showed the poorest performance.
2. The 400x400 image sets gave slightly better performance than the 256x256 image sets.
3. The results gave essentially no overall preference to the 256x256 or 512x512 transforms for 400x400 images.
4. Set 15 gave similar results to set 14, indicating that the two stage thresholding process used was a reasonable approximation to applying the entire detection algorithm with different K values.

The data indicate that a 400x400 image size may be slightly preferable to a 256x256 image size. The transform size is less critical, either size giving similar results. However the results are somewhat biassed due to the choice of data. As stated previously, the 400x400 image set was chosen from images which were at least 400x400. These images all contained relatively strong wakes at least 400 pixels long. The 256x256 images were then windowed from the

400x400 image, and hence were not a representative sample of wake images. It is to be expected that the performance would be slightly better for the 400x400 images, because the extra length will effectively improve the signal to noise ratio. If the whole range of wake lengths had been tested it is possible that the 256x256 image would have been more effective on shorter wakes.

TABLE 6-1

SIZE OPTIMIZATION DATA

400x400 Images, 512x512 Radon transforms

N	Bright Wakes		Dark Wakes		Envelope PD	Image FAR
	PD	FAR	PD	FAR		
4.0	.53	22.3	.26	4.6	1	27.0
4.5	.53	6.5	.20	0.3	1	6.8
5.0	.44	1.8	.20	0.2	.78	2.0
5.5	.40	0.8	.20	0.2	.78	1.0

256x256 Images, 512x512 Radon transforms

N	Bright Wakes		Dark Wakes		Envelope PD	Image FAR
	PD	FAR	PD	FAR		
4.0	.56	57.4	.23	11.8	1.0	69
4.5	.39	17.2	.23	1.6	.86	19
5.0	.30	7.4	.17	0.4	.71	8
5.5	.27	4.2	.17	0.2	.64	4

400x400 Images, 256x256 Radon transforms

N	Bright Wakes		Dark Wakes		Envelope PD	Image FAR
	PD	FAR	PD	FAR		
4.0	.43	4.5	.26	0.6	1.0	5.2
4.5	.43	1.7	.20	0.1	.93	1.8
5.0	.37	0.3	.20	0.0	.85	0.2
5.5	.33	0.2	.20	0.0	.85	0.2

TABLE 6-1 (cont'd)

SIZE OPTIMIZATION DATA

256x256 Images, 256x256 Radon transforms

N	Bright Wakes		Dark Wakes		Envelope PD	Image FAR
	PD	FAR	PD	FAR		
4.0	.45	6.1	.17	0.4	1	5.1
4.5	.35	2.6	.13	0.0	.80	2.0
5.0	.29	0.8	.13	0.0	.80	0.9
5.5	.26	0.3	.13	0.0	.73	0.4

256x256 Images, 256x256 Radon transforms

N	Bright Wakes		Dark Wakes		Envelope PD	Image FAR
	PD	FAR	PD	FAR		
3.0	.44	27.2	.33	16.0	1	43.0
3.5	.44	8.5	.24	2.8	.93	11.4
4.0	.37	3.3	.24	0.2	.93	3.5
4.5	.33	1.6	.17	0.1	.78	1.8

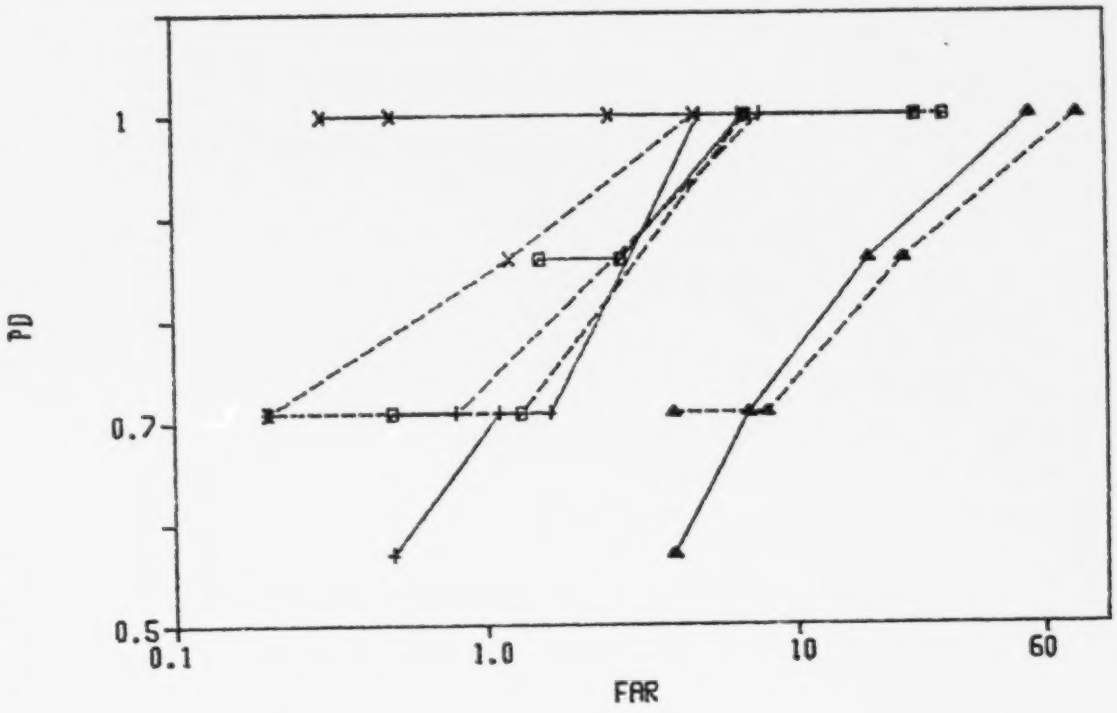

FIGURE 6-1

Ship detection performance curves for the size optimization tests.
The solid lines represent images containing ships.
The broken lines represent images containing wakes only.

□ 400x400 Images, 512x512 Transforms
Δ 256x256 Images, 512x512 Transforms
x 400x400 Images, 256x256 Transforms
+ 256x256 Images, 256x256 Transforms

7.0 STANDARD IMAGE SETS

It was decided, on the basis of the size research, to choose a standard set of 400x400 images for further testing. A set of wake and empty ocean images were windowed from the large SAR images provided by CRC. The empty ocean regions were chosen manually, using the following guidelines:

1. The region contained no visually detectable wake.
2. The region appeared to be uniform.
3. Where possible regions were selected from each side of visible wake components.
4. Regions were distributed uniformly over the image.
5. Regions did not overlap.

The wake images were chosen from the same images, which had been provided because each contained one or more ships and wakes. Two wake images were generally taken for each ship. One image included the ship and as much wake as would fit in the 400x400 window; the second image contained only the wake.

Details of each image in this set are contained in Appendix A.

8.0 BASELINE ALGORITHM

The baseline Radon transform and ADA were applied to the standard test image set to determine some of the characteristics of the transforms. The results were also used for comparison in determining effects of changes or additions to the algorithms.

8.1 DESCRIPTION

The 256x256 Radon transform of these images was taken. The clipped transform, with image mean subtracted, was used, with clipping level set at 160. The automatic evaluation algorithm was applied to the Radon transforms, with threshold 4σ.

8.2 TRANSFORM CHARACTERISTICS

This section describes some of the characteristics of the Radon transforms of the ocean and wake images. This includes the effect on the transform of features in the image, and the statistics of the transform elements.

8.2.1 Effect of Image Features

The transforms of uniform ocean areas showed few features, although the sinusoidal nature of the transformation of each image point was usually visible as sinusoidal 'streaking'. Features in the ocean images did affect the transform, the following were observed:

1. Bright points in the image were transformed to bright sinusoidal lines. Such points were produced by bright reflections from ships, as expected. Some wakes also appeared in the images as a string of bright points connected by distinguishable but less bright regions. These also produced a set of bright sinusoidal lines in the transform, all crossing at a single point defining the wake line.

2. One image showed parallel lines, apparently due to imaging of ocean wave features. This produced a vertical string of points in the transform.

8.2.2 Grey Level Statistics

The grey levels of the SAR ocean images have a Rayleigh distribution:

$$f(x) = (x/\alpha^2) \exp(-x^2/2\alpha^2) \quad x > 0$$

where f(x) is the probability that a pixel will have grey level x. An example of this distribution is shown in Figure 2-1.

It is expected that the transform statistics will have the following characteristics:

1. The mean of the transform grey levels should be zero, since the image mean has been subtracted from the pixels before doing the transform.

2. The standard deviation, σ, will depend on the lengths of the lines represented by the transform. If the original image grey levels were completely random, if each element of the transform consisted of a sum of N random points from the original image, and if no point in the original image was added into more than one transform element, then it can be shown that:

   $$\sigma = \text{constant} * \text{SQRT}(N)$$

   Where N is the number of pixels added in to the transform element. The actual relationship should be similar to this, although the conditions are not exactly satisfied.

8.2.2.1 Ocean Transform Statistics

The mean and standard deviations for the transforms of two ocean images were determined. The transform image contains a large area of blank 'background', representing lines which are completely outside the image area; this background was excluded when calculating the statistics and the histograms. The results are plotted in Figure 8-1 for one image, the other was similar. From the figures it can be seen that the distribution peak is higher and narrower than a Gaussian.

It was believed that this discrepancy was due to the variation of line lengths in the SAR image. Because this image is square, points in the transform corresponding to lines crossing the centre represent

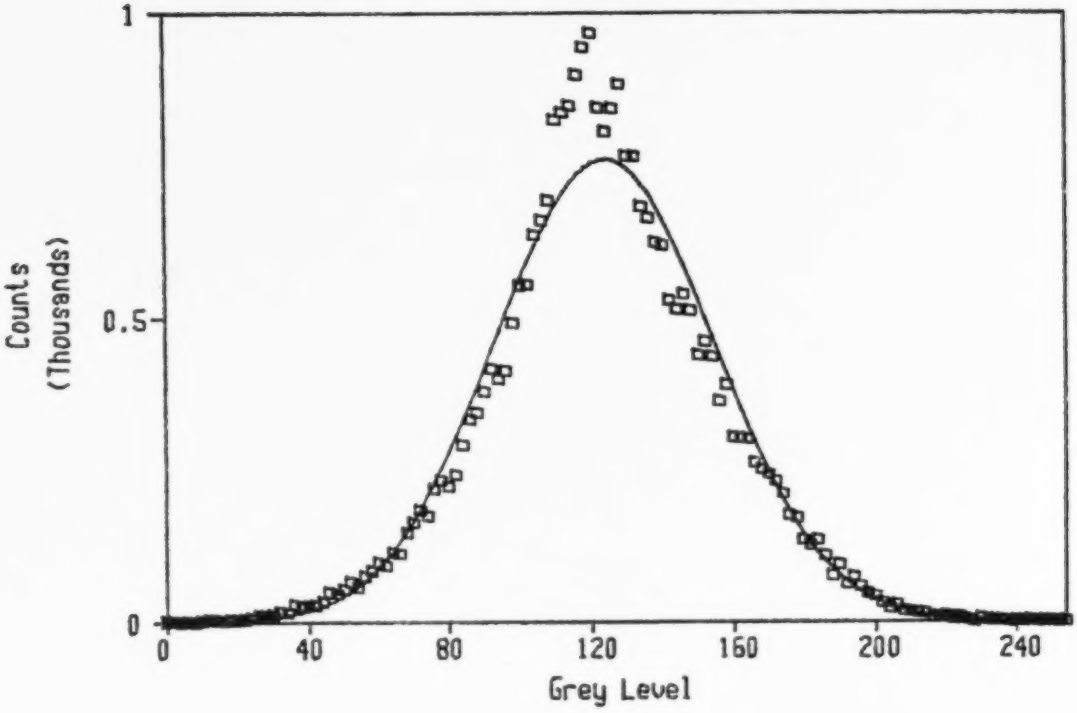

FIGURE 8-1

Grey level distribution for the Radon transform of image 9-s-1. The squares show the histogram, the line is a Gaussian fit to the data.

more pixels than points corresponding to lines crossing a corner. If, as stated above, the standard deviation depends on the line length N, then the combination of statistics from a range of line lengths will produce a distorted distribution.

To determine the actual number of pixels represented by each point the transform of a constant image, with grey level of 1, was taken. (The mean was not subtracted from the pixels when doing this transform.) The grey levels of this transform represent the number of image pixels summed into each transform pixel.

This length transform was then used to calculate the statistics of several sea images for various ranges of line lengths. The histograms have been plotted for two ranges of lengths for one of the images. The results are given in Figures 8-2, 8-3, and 8-4.

From these data it can be seen that the histogram appears to be a normal distribution, and the standard deviation initially increases with the length of the lines. However, instead of increasing proportionally to SQRT(N), the standard deviation appears to flatten out, or even decrease for long lines. No detailed study of this dependence was done, however it may have been due to contraventions of the assumptions made in deriving the square root relationship.

1. It was assumed that each image point is only added into one transform element. In fact each image pixel is added into 256 different Radon transform elements.

2. It was assumed that the initial image was random, and each pixel summed into the transform was chosen at random. In fact the elements lie along lines, and there may be correlations along lines, and between adjacent lines.

8.2.2.2 Ship Image Statistics

The statistics of two ship images, from regions adjacent to the empty ocean images previously measured, were then determined. The results for one are given in Figure 8-5, the second one was similar. Note that the Gaussian curve plotted in the figure is the empty ocean curve, it is not based on the statistics of the image containing the ship.

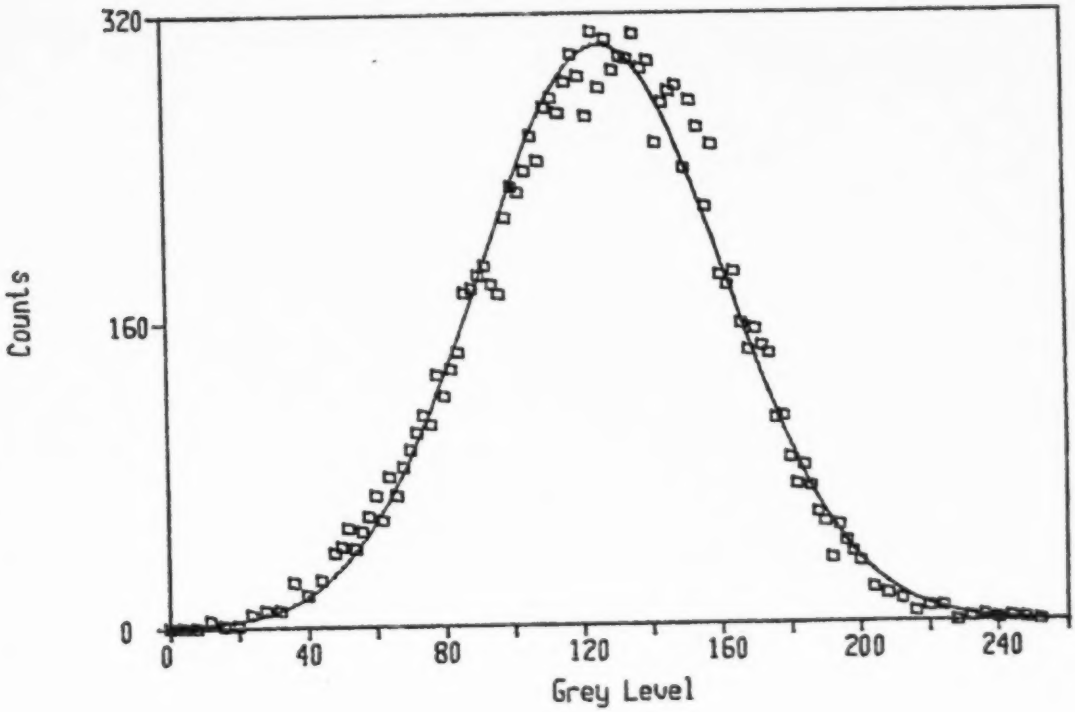

FIGURE 8-2

Grey level distribution for the Radon transform of image 9-s-1, for lines of length between 332 and 443 pixels. The squares show the histogram, the line is a Gaussian fit to the data.

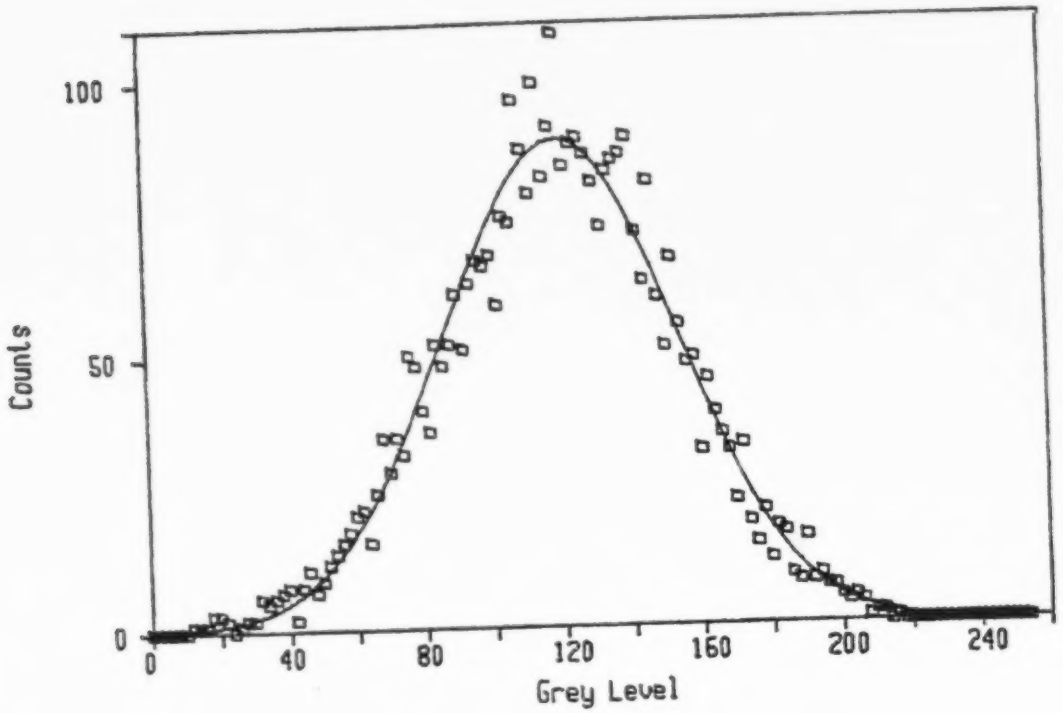

FIGURE 8-3

Grey level distribution for the Radon transform of image 9-s-1, for lines longer than 443 pixels. The squares show the histogram, the line is a Gaussian fit to the data.

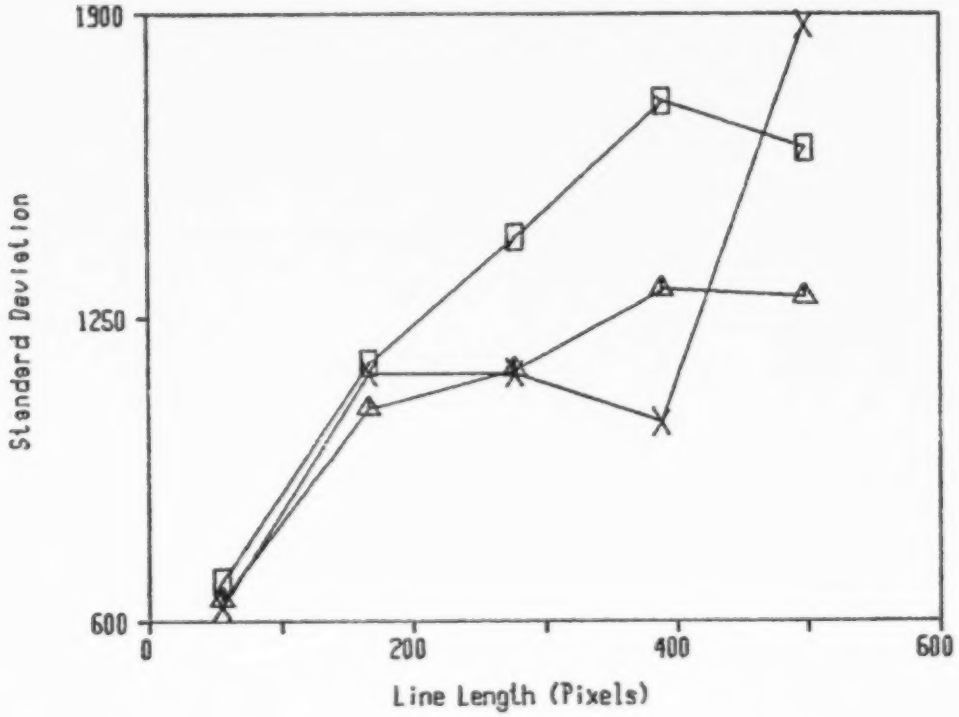

FIGURE 8-4

σ vs line length for image 9-s-1, 9-s-2, and 9-s-3. It can be seen that σ increases approximately as the square root of line length for lines up to 300 pixels long. For longer lines the dependence becomes erratic.

□ 9-s-1
Δ 9-s-2
x 9-s-3

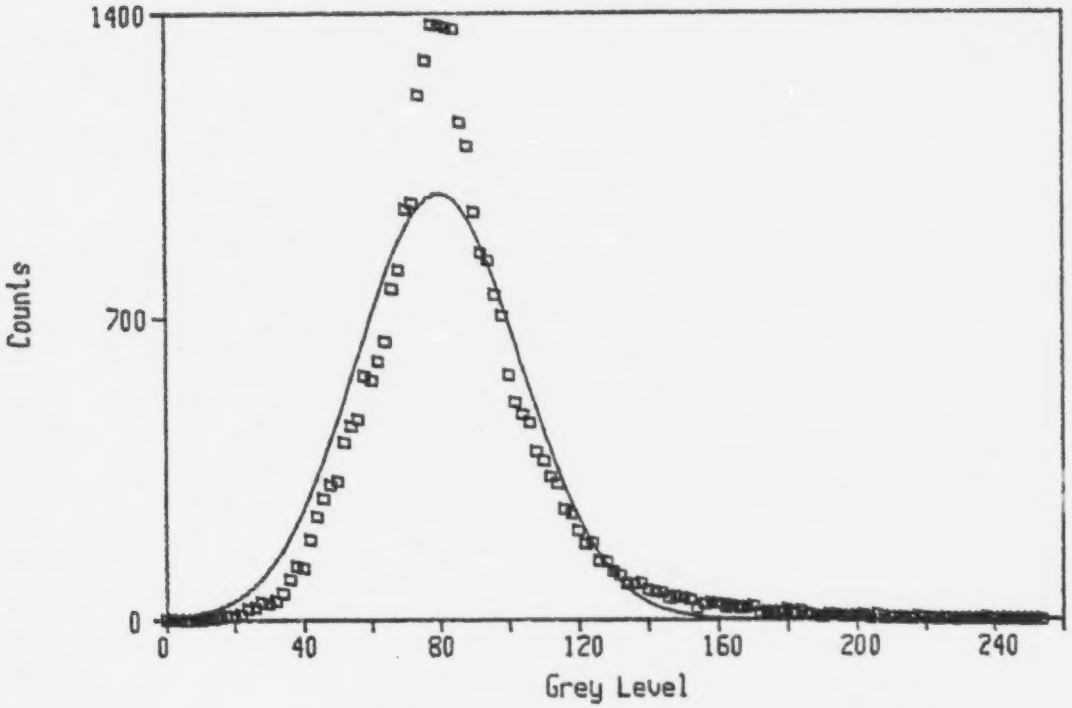

FIGURE 8-5

Grey level distribution for the Radon transform of image 9-v-3, containing a wake. The squares show the histogram data, the line is the Gaussian fit to image 9-s-1, the adjacent ocean image. Note that the Gaussian fit has been scaled to correct for the different values used in compressing the transform to 8 bits.

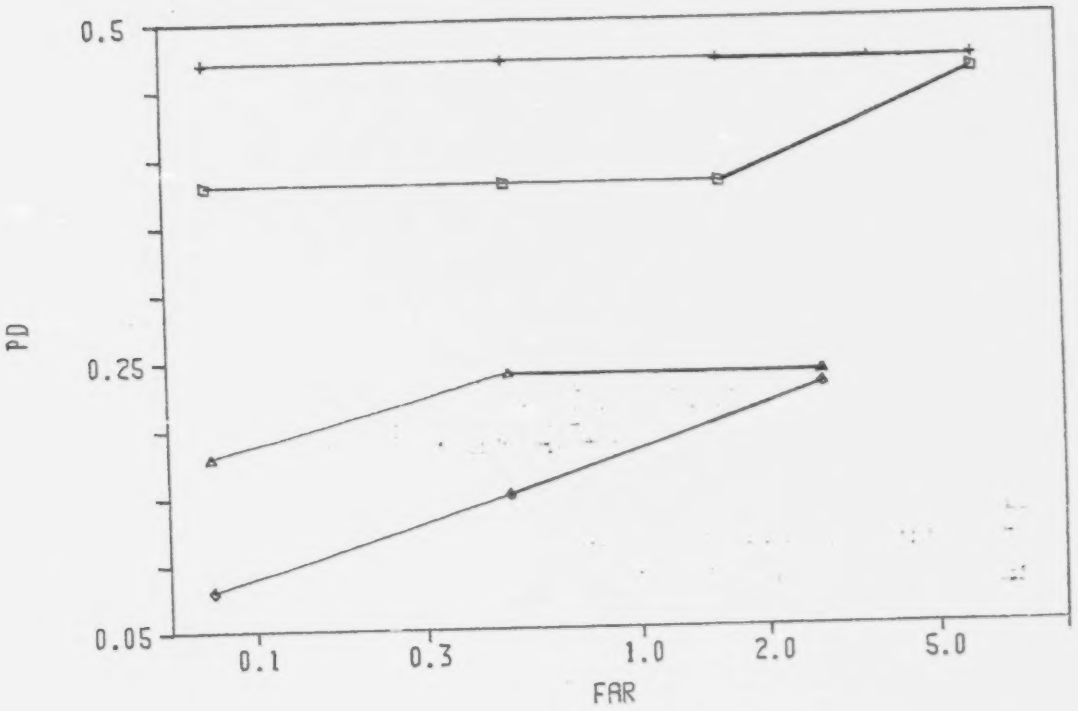

FIGURE 8-6

Performance curves for the baseline wake detection algorithm. The probability of detection (PD) for bright wakes and dark wakes is plotted against the false alarm rate (FAR). FAR is determined from the empty ocean transforms.

- □ Bright wakes, ship and wake images
- \+ Bright wakes, wake only images
- ◊ Dark wakes, ship and wake images
- Δ Dark wakes, wake only images

The ship image statistics were not determined as a function of line length, but they should not be significantly different from the empty ocean images, except for the changes produced by the ship and wake sections themselves.

8.2.2.3 Results

The above data lead to the following conclusions:

1. The empty ocean statistics can be used to predict the ship image statistics with reasonable accuracy.

2. The transform distribution is Gaussian for lines with a single length; the length variation in the lines causes the deviation from the Gaussian distribution.

3. The variation in standard deviation with line length is consistent with it being proportional to SQRT(N) where N is the number of pixels in the line, for short lines. As N increases beyond about 300 pixels the deviation becomes approximately constant.

8.3 ADA PERFORMANCE

The performance for the ADA on each image, and the overall FAR as a function of threshold, are given in Table 8-1 and Figure 8-6.

TABLE 8-1

BASELINE RESULTS

Empty Ocean Images

N	Bright Wakes		Dark Wakes		Image FAR
	PD	FAR	PD	FAR	
4.0		6.3		2.7	9.0
4.5		1.6		0.5	2.1
5.0		0.5		0.1	0.6
5.5		0.1		0.1	0.2

Images with Ships and Wakes

N	Bright Wakes		Dark Wakes		Envelope PD	Image FAR
	PD	FAR	PD	FAR		
4.0	46	8.2	23	0.0	1.0	8.2
4.5	.38	4.4	.15	0.0	.83	4.4
5.0	.38	1.9	.08	0.0	.83	1.9
5.5	.30	0.8	.08	0.0	.66	0.8

Images With Wakes Only

N	Bright Wakes		Dark Wakes		Envelope PD	Image FAR
	PD	FAR	PD	FAR		
4.0	.47	4.7	.24	0.0	1.0	4.7
4.5	.47	1.0	.24	0.0	1.0	1.0
5.0	.47	0.6	.18	0.0	1.0	0.6
5.5	.47	0.4	.18	0.0	1.0	0.4

8.4 COMPARISON OF ADA TO VISUAL EXAMINATION

The ADA detected about 50% of the wake components as bright wakes, and 25% as dark wakes. In order to determine if this performance was limited by the actual existence of peaks due to the components a visual examination was made of the transforms. This determined if peaks existed for the remaining wake components, and why the ADA failed to detect these components.

8.4.1 Procedure

The standard image set was used for this study. Each image, its ground truth, and its Radon transform were displayed on the IMAVISION. The components detected by the ADA were identified. A visual examination of the Radon transform was then made to see if there were peaks corresponding to the undetected components. If such peaks were found the reason for the ADA failure was determined.

8.4.2 Results

Table 8-4 gives the observations for each image. The ADA detected 21 of the 30 wake components (note that this is combining bright and dark wave detections), for an overall PD of 0.7. Visual examination detected 29 components, for an overall PD of .96. The ADA failed to detect wake components for four reasons:

1. The peak was below the 4σ threshold (5 components).

2. The peak was combined with a peak due to another component (2 components).

3. The peak was combined with a false alarm peak (1 component).

4. There was no visually detectable peak produced (1 component).

The results show that the ADA performance was not limited by the existence of peaks in the transform, but rather by its failure to detect such peaks. In particular a lower threshold should improve the performance considerably. Simply lowering the threshold in the current algorithm would probably not be sufficient, since it would increase the false alarm rate and would combine more adjacent peaks. It would probably be necessary to produce an improved ADA, using local peak detection and/or other methods to detect all the peaks and eliminate false alarms.

TABLE 8-4

COMPARISON OF ADA AND

VISUAL PEAK DETECTION

Image	Wake Comp.	Wakes (ADA)	Wakes (Vis)	Comments
9-v-1	2	1	2	Peaks were combined.
9-v-2	2	1	2	Threshold was too high to detect second peak.
9-v-3	1	1	1	
9-v-4	1	1	1	
10-v-1	2	2	2	
10-v-2	2	2	2	
10-v-3	2	2	2	
10-v-4	1	1	1	
10-v-5	2	1	2	Second peak was combined with false alarm peak.
10-v-6	2	1	2	Second component was below the threshold.
11-v-1	3	1	2	Second peak was combined with first peak. There were no visually detectable peaks associated with the third component.
11-v-2	3	2	3	Third component produced bright and dark peaks, but both were below ADA thresholds.
11-v-3	4	2	4	Third and fourth components were below ADA threshold.
11-v-4	3	2	3	

8.5 ADDITIONAL TESTING

The baseline transform was run on the additional image set, to obtain more data on its performance, using an independent set of images. The results are summarized in Table 8-5. They are generally similar to the baseline results. The differences are probably due to random variation between the image sets.

TABLE 8-5

ADA PERFORMANCE FOR ADDITIONAL IMAGE SET

Empty Ocean

N	Bright Wakes		Dark Wakes	
	PD	FAR	PD	FAR
4.0		3.2		1.8
4.5		.85		.49
5.0		.49		.12
5.5		.24		0
6.0		0		0

Ships and Wakes

N	Bright Wakes		Dark Wakes	
	PD	FAR	PD	FAR
4.0	.58	4.0	.26	.24
4.5	.42	2.0	.21	0
5.0	.32	1.5	.16	0
5.5	.32	.6	.16	0
6.0	.32	.4	.16	0

9.0 NORMALIZED EMPTY OCEAN ADA

The Radon transform statistics discussed previously showed that elements representing image lines having approximately the same lengths have grey intensities with approximately a Gaussian distribution. The width of the distribution increases approximately as the square root of the line length, at least for lines up to about 300 pixels long. The research described here was done to determine if the automatic detection algorithm could be improved by using this knowledge.

The baseline ADA measured the mean and standard deviation of the Radon transform, and used thresholds of mean +/- Nσ to produce bitmaps of the bright and dark areas in this transform. It then found the minimum or maximum in each connected bright or dark area, and took it as representing a line in the original image. The following modifications were considered to improve the ADA:

1. Use statistics from an adjacent empty ocean transform to determine the thresholds. This should make the thresholds more accurate, since the statistics would not be affected by wakes in the image being analysed.

2. Use different thresholds for different line lengths. This will correct for the variation in transform statistics with line length. It may also make the ADA performance less dependent on the position of the wake in the image; currently a wake cutting across the corner of the image is less likely to be detected than one going through the middle, because of the length difference.

It was decided to combine these modifications to produce a single modified ADA for testing.

9.1 EMPTY OCEAN CHARACTERIZATION

An empty ocean background region was chosen for each region being analyzed. The regions were the same size, and had similar characteristics; the only difference was that the empty ocean region did not contain any visible wakes. The choice was made by visual examination and by comparing the image statistics for the regions; in an operational system the background region would be selected automatically, presumably from areas already examined for wakes.

9.2 NORMALIZATION METHOD

The Radon transforms for the wake and background regions were computed, producing the search transform and the background transform. The statistics (mean and σ) for the background transform for line lengths between 100 and 150 were then measured. The search and background transforms were usually scaled differently, so that they both had a range of 0 to 255; the background mean and σ values were therefore rescaled to match the scaling used for the search transform.

The search transform was then normalized to line length using the formula:

$$f_S = 127 + (f - m_S)/SQRT(0.15L)$$

where L is the length of the line associated with the element, f is the element grey level, m_S is the rescaled mean, and f_S if the normalized transform element.

These normalized values represented the 'distance' of the transform element from the mean, relative to the expected range of distance for elements representing that line length. The normalized values were scaled to be centred around 127, the number 0.15 was an adjustable scaling factor that was chosen to make the values fall in a range between 0 and 255.

Once the search transform had been normalized to line length the threshold was calculated:

$$Delta = 4*(\sigma_S)/SQRT(125)*0.15)$$

$$Threshold = 127 +/- Delta$$

Delta thus corresponded to the 4 σ threshold used in the baseline ADA; it was scaled to the average line length of 125, and the factor of 0.15 corrected for the 0.15 scale factor used in the previous step. The transform was thresholded and the peak element in each region was found, using the same steps as were used in the baseline ADA.

9.3 RESULTS

This modified ADA was applied to the baseline image set. These had already been transformed, so it was only necessary to implement and run the detection algorithms. The results of the tests are summarized in Table 9-1 and Figure 9-1.

The empty ocean FAR for the normalized ADA was higher than that for the baseline ADA, for N=4.0 and 4.5. The additional false alarms are all in two images, 9-s-4, and 11-s-3. Image 9-s-4 consisted of two regions of distinctly different brightness, and was obviously anomalous. This anomaly did not affect FAR for the baseline ADA, since sigma is increased and hence the thresholds were automatically increased to compensate for the non-uniformity. In the normalized ADA sigma was taken from an adjacent, uniform region, and hence the thresholds were smaller. This produced a large number of bright and dark false alarms. Image 11-s-3 was not obviously anomalous by visual examination. Most of the false alarms were at levels close to the N=4 or 4.5 threshold and this may indicate the adjacent region was different enough to produce a threshold slightly too low. When these two images were removed from the set the resulting false alarm rates were generally lower than those from the baseline ADA.

PD for the normalized ADA was similar to that for the baseline ADA, the sample size was too small to detect any significant differences. The PD/FAR curves have been plotted including FAR from the anomalous images in Figure 9-1.

TABLE 9-1

NORMALIZED DETECTION SYSTEM PERFORMANCE

Oceans Only

N	Bright Wakes		Dark Wakes	
	PD	FAR	PD	FAR
4.0	-	11.7	-	5.1
4.5	-	3.4	-	2.1
5.0	-	0.5	-	0.6
5.5	-	0.4	-	0.4
6.0	-	0.0	-	0.0

Images with Ships and Wakes

N	Bright Wakes		Dark Wakes	
	PD	FAR	PD	FAR
4.0	.31	21	.31	22
4.5	.31	8	.31	6.8
5.0	.31	3.8	.15	2.5
5.5	.31	2.5	.15	1.4
6.0	.08	1.1	.08	1.1

Images with Wakes Only

N	Bright Wakes		Dark Wakes	
	PD	FAR	PD	FAR
4.0	.65	17	.18	15.8
4.5	.53	6.8	.18	4.7
5.0	.53	3.5	.12	2.5
5.5	.29	2.7	.12	0.6
6.0	.24	1.6	.12	0.6

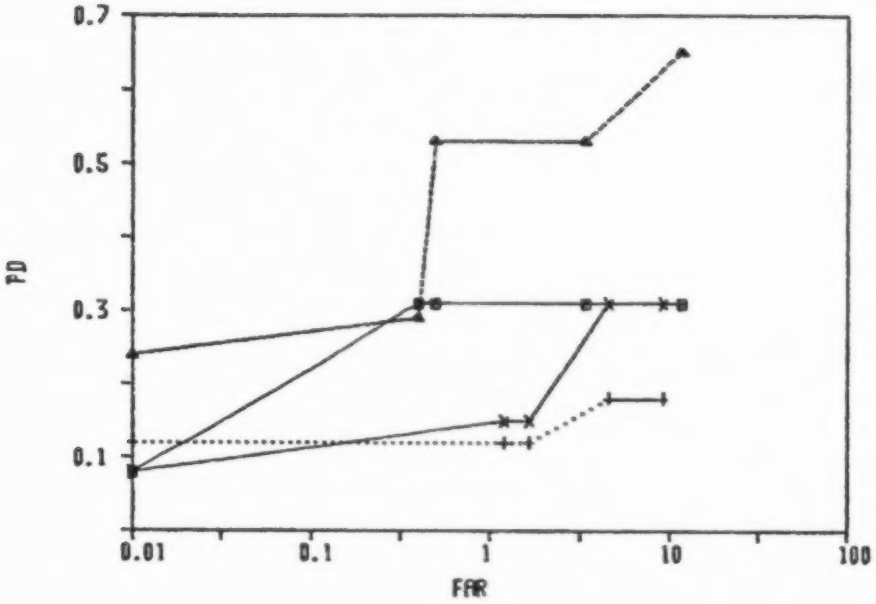

FIGURE 9-1

Performance curves for the normalized wake detection algorithm. The probability of detection (PD) for bright wakes and dark wakes is plotted against the false alarm rate (FAR). The FAR is determined from the empty ocean transforms.

□ Bright wakes, ship and wake images
Δ Bright wakes, wake only images
x Dark wakes, ship and wake images
+ Dark wakes, wake only images

10.0 PEAK SHAPE MEASUREMENT

10.1 LOCAL SIGMA

Visual examination of Radon transform peaks indicates that the peaks due to wakes are often formed by the crossing of a number of bright lines, forming a 'bow tie' shape. False alarm peaks tend to have smoother surroundings. Tests were done to determine if this difference could be used to differentiate detections from false alarms.

The best method of differentiating false alarms from wake peaks might be to actually recognize the 'bow tie' shape of the peak. This would be complicated to implement, so for initial testing purposes a simpler method was used. The standard deviation, σ_ω, of a square window surrounding the peak, but not including the peak pixel, was used. It was expected that this would be larger for wake peaks than for false alarm peaks.

An algorithm was developed to read the ADA output file to find the peak positions. It then found the mean and standard deviation for the pixels in the NxN square surrounding the peak pixel, but not including this pixel. N was adjustable, a value of 5 was used. The routine was applied to all of the transforms in the baseline set.

The Radon transforms had all been scaled to a range of 0-255. In order to compare results the values of the mean and standard deviation for each peak were scaled back to the original radon transform range.

10.1.1 Results

Examination of the results indicated that σ_ω was larger for wakes than for false alarms, and that a threshold value of 2000 would be a reasonable choice to separate them. The detections and false alarms were determined manually using this threshold, the results are given in Table 10-1. This indicates that for bright wakes the PD is unchanged, while FAR is reduced by factors of 2 or more. Dark peak false alarms were reduced for empty ocean images. There were none in the ship images.

The process appears to improve the system significantly, however the improvement is only marginally better than that obtained using a higher (4.5σ) threshold in the baseline ADA.

TABLE 10-1

LOCAL SIGMA THRESHOLD RESULTS

Bright Wakes

	PD		FAR	
	Baseline	Thresholded	Baseline	Thresholded
Empty Ocean	-	-	6.3	1.2
Ships+Wakes	.46	.46	8.2	4.4
Wakes Only	.47	.47	4.7	1.2

Dark Wakes

	PD		FAR	
	Baseline	Thresholded	Baseline	Thresholded
Empty Ocean	-	-	2.5	0.3
Ships+Wakes	.23	.23	0	0
Wakes Only	.24	.24	0	0

10.2 BOWTIE SHAPE RECOGNITION

The results using the local sigma measurements suggested that a more sophisticated algorithm to recognize the bowtie shape and differentiate wakes from false alarms should be developed.

10.2.1 Algorithms

Two shape measurement algorithms were developed and tested, bowtie_1 and bowtie_2.

10.2.1.1 Bowtie_1

This algorithm used a template to detect the bowtie shape. The template is shown in Figure 10-1. It produces a measure of image brightness for each of 8 triangular segments surrounding the peak.

If the peak has a bowtie shape then the sum along the axis should be large, and the sum perpendicular to it should be small. The algorithm measures this difference by taking the largest sum, and subtracting the smaller of the two perpendicular sums, to get the difference, D1. This difference depends on the scaling of the Radon transform; to remove this dependence it is divided by the previously measured standard deviation of the transform. This produces a measure of the visibility, V1, of the bowtie shape compared to the overall variation in the image.

$$v1 = D1/\sigma$$

10.2.1.2 Bowtie_2

This is similar to bowtie_1, but uses a different template; as shown in Figure 10-1. This averages two pixels on each side of the peak for each of six directions; it therefore has more precise directions than bowtie_1, and does less averaging. The algorithm found the maximum strength direction, Maxdir, the minimum strength direction, Mindir, and the difference from the peak height for each, Maxdiff and Mindiff. (Directions varied between 1 and 6.)

```
7  8  8  8  8  8  1  1  1  1  1
7  7  8  8  8  8  1  1  1  1  2
7  7  7  8  8  8  1  1  1  2  2
7  7  7  7  8  8  1  1  2  2  2
7  7  7  7  7  8  1  2  2  2  2
6  6  6  6  6  P  2  2  2  2  2
6  6  6  6  5  4  3  3  3  3  3
6  6  6  5  5  4  4  3  3  3  3
6  6  5  5  5  4  4  4  3  3  3
6  5  5  5  5  4  4  4  4  4  3
```

Bowtie_1

```
   6 1 2
5       3
4   P   4
3       5
   2 1 6
```

Bowtie_2

FIGURE 10-1 TEMPLATES FOR BOWTIE_1 AND BOWTIE_2.

The template is placed over the image, with the centre point, P, at the peak being analyzed. The sum of the pixels in each numbered segment of the template is then found.

10.2.2 Results

Bowtie_1 was found to be quite effective for correctly identifying strong peaks (height greater than 250) found by the baseline ADA. It is not so effective in identifying less strong peaks, although it did separate many of the false alarms.

It was found that the results from bowtie_2 could be used to identify less bright peaks; the wake peaks tended to have the following characteristics:

1. maxdir - mindir = 3 or

2. (Maxdiff - Mindiff) > 3.

That is the strong and weak directions tended to be at right-angles, and the difference in their strengths was large.

These results were put into a simple set of rules for classifying the peaks detected by the ADA; these are listed below. The rules are applied one at a time in the order indicated, to each peak detected by the ADA, until the peak is identified as a wake or a false alarm.

1. If the peak has V1 less than 40 it is a false alarm.

2. If the peak height is greater than 250 it is a wake.

3. If (MaxDir - Mindir) = 3 (at right-angles), and MaxDiff/MinDiff is greater than 3, it is a wake.

4. If bowtie_2 gives (MaxDir - MinDir) = 2, and MaxDiff/MinDiff is greater than 4, it is a wake.

5. The peak is a false alarm.

These rules were applied to the baseline image set. The results are summarized in Table 10-2.

The same algorithms were applied to the dark peaks. The smaller number of dark peaks meant that the statistics were considerably worse, so no different rules were developed for them. Instead the rules that were applied to the bright peaks were modified appropriately and applied to the dark peaks. The rules are listed below; the results are given in Table 10-2.

1. If the peak has V1 less than 40 it is a false alarm.

2. If the peak height is less than 6 it is a wake.

3. If bowtie_2 gives (MaxDir - Mindir) = 3 (at right-angles), and MaxDiff/MinDiff is greater than 3, it is a wake.

4. If bowtie_2 gives (MaxDir - MinDir) = 2, and MaxDiff/MinDiff is greater than 4, it is a wake.

5. The peak is a false alarm.

These results show a strong decrease in FAR. It should be noted, however, that the Bowtie detector was trained on the same images that it was tested on; so the measured performance is probably better than would be obtained on an independent sample.

TABLE 10-2

BOWTIE SHAPE DETECTION

	Bright Peaks		Dark Peaks	
	PD	FAR	PD	FAR
Empty Ocean		0.1		0.3
Wakes Only	.41	0.4	.17	0
Ships and Wakes	.46	2.0	.23	0

11.0 SEMBLANCE

The semblance provides a statistical measure of the local variation in the SAR image grey level, and may be useful in distinguishing wakes from background ocean (Stoffa, 1981). This section describes research on using the semblance for wake detection.

Semblance is defined as:

$$S = \frac{(\sum_w g)^2}{N \sum_w g^2}$$

where g is a sample value (the pixel grey level)
w is the region or window the sum is taken over
N is the number of samples in the window.

The semblance can also be defined or calculated as the square of the mean divided by the mean of the squares, where both means are calculated in the given window.

Semblance is a second order statistic and is a measure of the amount of variation in the samples. However, unlike other second order statistics such as variance and standard deviation, semblance is normalized to a range between 0 and 1 and the definition does not require that the mean be subtracted from each sample. A semblance of 1 implies perfect uniformity of the samples or no variation; a semblance close to 0 implies a great deal of variation.

Semblance is invariant over a multiplicative scaling, but varies quite strongly with an additive scaling. For example if most of the samples in the chosen window are small, one large value will cause the semblance to drop drastically, whereas if most of the samples have large values, one small value will not greatly affect the semblance.

These characteristics make the choice of image scaling very important. Since it is necessary to emphasize features which are generally darker or lighter than the background, subtracting the overall image mean from each sample will cause both dark wakes and bright wakes to have values differing greatly from zero. Their semblances will not be strongly affected by a few speckles of a different brightness. On the other hand, an area with values

close to the image mean would have to be extremely uniform to have a semblance close to one. This scaling may, therefore, aid in the detection of distinct wakes but obscure weak wakes.

11.1 SEMBLANCE FILTER PREPROCESSOR

The simplest method of applying the semblance is to use a square semblance filter to preprocess the image. The filtered semblance can be used directly as the input to the transform or the semblance image can be multiplied by the original image, and then transformed. If the semblance is larger for a wake pixel than for a background pixel then multiplying the image by the semblance will enhance bright wake pixels. Dark wake pixels will be brought nearer to the background grey level, so these wake components will be less detectable.

11.1.1 Algorithm Implementation

The semblance filter preprocessor was implemented on the IMAVISION. It could calculate the semblance over any size rectangular window up to 11x11. The output was scaled to a range of 0 to 255.

Four processing steps were used to detect the wakes using the semblance:

1. A 3x3 semblance filter was applied to the images.

2. The resulting filtered images were multiplied by the original images, on a pixel by pixel basis.

3. The Radon transform was applied to the resulting product. The clipping transform was used, with the threshold set at 160.

4. The transform was put through the automatic evaluation algorithm.

11.1.2 Results

The preliminary image set was processed using this procedure. Visual examination of the transform indicated that the 3x3 semblance did little to enhance wakes. The wakes were less visible in the semblance image than in the original, and no improvement was seen in the product of the original image times the semblance image.

The ADA performance was given in Table 5-1, with the other preliminary results. The data show no improvement in detection of bright wakes due to application of the semblance preprocessor. The PD and FAR are essentially identical to those for the same images in the clipped set.

The dark wake PD decreased from 0.18 to 0.12. This represented a change from 3 to 2 detected wake components, and may not have been statistically significant. The change was likely due to the multiplication of the image and the semblance, as discussed above.

This square semblance filter may not have been effective because its shape did not correspond to the wake shape. Thus if it was large enough to detect a uniform region along a wake then it was so wide that it saw a non-uniform region across the wake, so that the wake had little effect on the semblance.

11.2 SLANT STACK TRANSFORM

The Radon transform sums all the pixels along a line crossing the image into a single transform element. The slant stack algorithm replaces this sum with the semblance of these pixels. Thus it produces a transform which is similar to the Radon transform, but with elements showing the variability along each line in the image. If the variability between a wake and the ocean background differs then the difference should appear in the slant stack transform.

The Radon transform algorithm was modified to calculate the slant stack transform. The image mean was subtracted from each pixel before doing the transform, so the slant stack measured the variation of the data from the mean. The algorithm was applied to the preliminary image set. The resulting transforms were not promising; the wakes were less visible than they were in the original images, and in many cases had completely disappeared. This may have been because the algorithm measured semblance across the entire image, and the wake components were not uniform across this length. On the basis of this preliminary research it was decided not to pursue the slant stack algorithm any further.

11.3 DIRECTIONAL SEMBLANCE PROCESSING

The semblance preprocessor filter, and the slant stack transform were both tried on images, with little success. The Directional Semblance Filter (DSF) is a generalization of these algorithms. It determines the semblance for a set of long narrow windows centred on each pixel, and covering the entire range of directions. It can be combined with a Radon transform to produce an output similar to that of the basic Radon transform, but containing more directional information.

11.3.1 Definition

The DSF is defined as follows:

$$S(k,l,D) = \left[\sum_{W(d)} f(i,j)\right]^2 / \left(N \sum_{W(d)} [f^2(i,j)]\right)$$

Where W(d) is a window in the image centred at (k,l) and lying along a direction defined by d. For example for d=45 degrees:

$$W(d) = \begin{matrix} 1 & 0 & 0 & 0 & 0 \\ 0 & 1 & 0 & 0 & 0 \\ 0 & 0 & 1 & 0 & 0 \\ 0 & 0 & 0 & 1 & 0 \\ 0 & 0 & 0 & 0 & 1 \end{matrix}$$

The DSF reduces to the slant stack in the case where a long thin window (long enough to cross the entire image) is used; it reduces to the semblance when a rectangular, non-directional window is used.

11.3.2 Initial Testing

In order to determine if the concept showed promise the directional semblance was calculated at chosen points in a few images. These points were taken along both bright and dark wakes and in background ocean. Using an 11x11 neighbourhood, there appeared to be very little difference in the semblance between wakes and background; and the semblance along the known direction of a wake was not always greater than in any other direction.

Using a 22x22 window had much better results. Dark wakes had maximum directional semblances between 0.46 and 0.89 with the maximum usually occuring in the known direction of the wake. Bright wakes had

maximum semblances between 0.74 and 0.83, again with the maximum usually occuring in the known direction of the wake. Background maximum semblances were between 0.38 and 0.47 with the maximum generally occuring in the horizontal direction (to the eye the background ocean appears to be made up of many short horizontal lines).

Algorithms were then developed to apply directional semblance filters to the test images. When the filtered images were displayed, the wakes were noticeably enhanced by the filter with direction closest to the wake direction and were noticeably blurred by the perpendicular filter. When one of these images was processed by the Radon transform (the vertical filter applied to an approximately vertical bright wake) the visible bright wakes showed up as distinct peaks and were also easily detected by the automatic detection algorithm with no false alarms. This was an improvement over the detection and false alarm rate performance for the original image.

11.3.3 DSF System Implementation

The initial tests indicated that the DSF might be quite useful for wake detection, and a complete DSF and Radon transform process was implemented for detailed testing. Directional semblance algorithms were developed to filter the image by the calculation of the semblance under a user-defined mask within a user-defined neighbourhood around each pixel. A constant (usually the image mean value) was subtracted from each pixel prior to calculating the semblance. Output semblance values were scaled between 0 and 127, and set in a range so that dark wakes stayed dark, bright wakes stayed bright and background tended to be middle grey. Four separate masks were defined so that four different directional semblances could be calculated in a single pass. Each input pixel (except near the edges) produced four output semblance values which were put into separate images.

In order to completely test the directional semblance it was necessary to process the filtered images using the Radon transform. The filters each enhance lines going in a different direction. The transform can be applied to each enhanced image to produce four transforms, in which the corresponding directions have been enhanced. These must be combined for

evaluation, by choosing the area from each transform representing lines in the enhanced direction. The ADA can then be applied to the combined transform. The overall process chosen to do this was as follows:

1. The directional semblance filters were applied to an image, to produce four filtered images.

2. Each of the four filtered images was transformed using the standard Radon transform, with the image mean subtracted.

3. All four Radon transform images were rescaled to a common grey scale (0 to 255).

4. The four Radon transforms were combined into one by using only the angle ranges of the RT closest to the direction of the directional filter applied.

5. The automatic peak detection algorithm was applied to the combined transform and the results evaluated.

In order to get more information on the performance of the directional semblance algorithms a second evaluation method was introduced. This required measuring the height of the peak, that is the actual value of the element. Since the same peak would appear from different processing methods, its height is a measure of how much the processing has improved its detectability.

11.3.3.1 Processing Details

The specific methods used to implement the directional semblance filter and combine the Radon transforms are described in this section.

The semblance value is always between 0 and 1; these are scaled to produce the filtered image with a 0 to 255 grey level range. It was decided to keep bright pixel and dark pixels distinguishable. The semblance values for bright pixels (grey level greater than the image average) were scaled between 127 and 254, those for dark pixels were scaled between 127 and 0. Thus a bright pixel with a directional semblance of 1 would be scaled to 254 in the output image, a dark pixel with semblance 1 would be scaled to 0.

To combine the Radon transforms of the four filtered images into one, two methods were proposed:

1. Cut and paste the 45 degree range of each of the four Radon transforms which were closest to the direction of the filter used to produce the image.

2. Cut and paste the 90 degree range of each pair of Radon transforms corresponding to perpendicular filter directions, then combine the two resulting Radon transforms by averaging.

   These methods are illustrated in Figure 11-1.

11.3.3.2 Filter Definition

A number of specific filters and combination methods were chosen for preliminary investigation.

1. Filter A - This is a set of four directional semblance filters operating in a 22x22 pixel neighbourhood around each pixel. Semblance is calculated acording to the formula described in Section 11.3.1. The actual directional masks used within the neighbourhood were lines 2 pixels wide and 22 pixels long in each of four directions: (|-\/). The two pixel width allowed the diagonal lines to be the same real length as the vertical and horizontal lines and to have the same number of pixels (44).

2. Filter B - This set of filters used the same neighbourhood and directional masks as Filter A, but after calculating the semblance values, each pair of perpendicular directional values are compared and only the maximum value is kept, the other being set to the neutral value of 127. For example, if the vertical semblance is 234 and the horizontal semblance is 216, the output values will be 234 and 127 respectively. This local wake detection should reduce the contribution of a wake in one direction to false alarms in perpendicular directions.

3. Filter C - This is a set of filters similar to Filter A but in a 21x21 pixel neighbourhood, and with the directional masks reduced to one pixel in width. This has the result that the diagonal masks are actually longer than the vertical and horizontal masks since the number of pixels in all masks was 21.

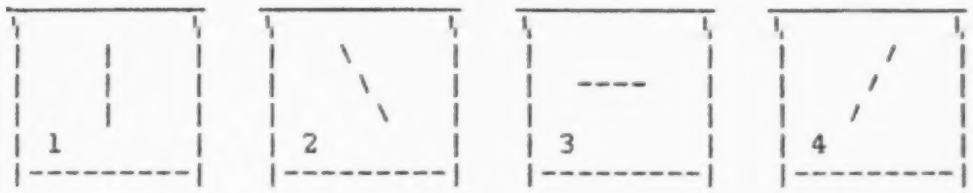

(A)

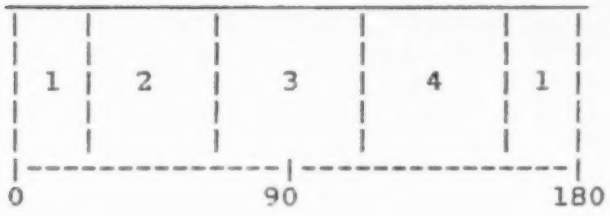

(B)

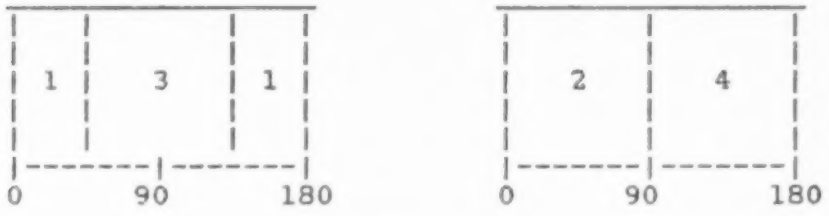

(C)

FIGURE 11-1

Combination of semblance filters:

(a) The filters produce four images, each emphasizing one of the four directions defined here.
(b) Combining the images by cutting and pasting the 45 degree range closest to each direction.
(c) Combining the images by cutting and pasting the 90 degree range closest to each perpendicular direction into two images. The two images are then averaged.

4. Filter D - This set of filters is similar to Filter C but in a 15x15 pixel neighbourhood and each mask being a 15x1 pixel line.

5. Filter E - This set of filters is similar to filter B in using only the maximum of each pair of perpendicular values; but uses the same directional masks as Filter D.

11.3.4 Preliminary Investigation

The directional semblance processing was evaluated as usual, by measuring the PD and FAR rates using the ADA. To get more information on the effect of the filtering the peak heights were also measured; if the filtering was useful these heights should increase.

A small set of test images was used for the initial evaluation, consisting of three images containing bright wakes, three images containing dark wakes (two of which also contained bright wakes); and two images of empty sea. These were all taken from the standard image set.

The data from this preliminary investigation will not be presented, only the results will be given. The data for those filters chosen for detailed investigation is included in results from that investigation.

11.3.4.1 Transform Combination Methods

Both methods of combining the Radon Transforms described in Section 11.3.3.1 were applied, and the results from the peak detection were compared. This indicated the following:

1. The averaging method usually had stronger peaks for real wakes, and thus should have a greater PD.

2. The averaging method had a FAR of about half that for the cut and paste method.

3. The averaging method produced generally smaller false alarm peaks.

The method of averaging the pairwise combined Radon transforms was therefore better than the simple cut and paste method since it generally emphasized wake peaks and de-emphasized false alarm peaks. This

resulted in a higher probability of detection and a lower false alarm rate. The averaging method was used exclusively in all further research requiring combination of Radon transformations of directionally filtered images.

11.3.4.2 Comparison Between Filtered and Unfiltered Images

This section compares performance for images processed by the method described in Section 11.3.3, and images not filtered by the semblance filters.

Comparison of peak heights for detected wakes indicated that the semblance filtering enhanced dark wakes but degraded very bright wakes. Faint bright wakes were not degraded and in some cases were actually enhanced.

Semblance filtering was found to increase the false alarm rate. The main reason for this was that the semblance filtering drastically increased sensitivity to dark lines, so the detection algorithm saw many more dark lines which were not associated with wakes.

The results from the preliminary tests were used to decide which of the five semblance filters tested had the best performance. The purpose was to select two filters for further testing on a larger set of images with a variety of peak detection algorithms. Filters D and E were selected since they appeared to have the best overall performance on bright and dark wakes respectively.

11.3.5 Detailed Evaluation of Selected Filters

Filters D and E were applied to the entire standard image set. The results given here include the results from the subset of images used for preliminary testing.

The performance is summarized in Table 11-1. The results from the baseline processing, without the semblance filters, are also given in Table 11-1 for comparison.

TABLE 11-1

COMPARISON OF RESULTS

	Baseline	Filt D	Filt E
Empty Ocean Images			
Bright Wake FAR	6.3	7.8	4.5
Dark Wake FAR	2.7	8.9	7.5
Images Containing Ships and Wakes			
Bright Wake PD	.46	.53	.53
Dark Wake PD	.23	.31	.31
Images Containing Only Wakes			
Bright Wake PD	.47	.65	.59
Dark Wake PD	.24	.18	.18
Peak Characteristics for All Images			
Bright Peaks			
Average wake peak height	8.23	6.72	6.54
Maximum False Alarm peak height	6.04	5.99	5.53
Dark Peaks			
Average wake peak height	-5.84	-7.84	-7.91
Maximum False Alarm peak height	-6.04	-7.37	-6.67

11.3.6 Results

The semblance filtering process was used to try to emphasize wakes by using the expected property of uniformity along their length. It was thought that this would be most effective for enhancing dark wakes, which are generally more uniform than bright wakes. The results indicate that bright wake detection is improved by the semblance filtering, dark wake detection was improved for images containing ships but decreased for images containing only wakes. The peak heights were increased for dark wakes and decreased for bright wakes.

This unexpected result may be statistical fluctuation due to the small sample size. It is also possible that it is an effect of the detection algorithm. The increased number of dark false alarms may obscure dark wake peaks, and cause the detection algorithm to miss them. Weak bright wakes may be enhanced by the semblance and detected, while strong bright wakes are not degraded enough to be missed, resulting in a net increase in bright wake PD.

11.4 NORMALIZED DIRECTIONAL SEMBLANCE

The process of normalization to line length and comparison to adjacent empty ocean areas was applied to the directional semblance filter data. No study of the statistics of the processed transforms was made, the technique used to apply the normalization process to the baseline system was repeated for the semblance data. That is the radon transform bins were divided by the square root of the number of image pixels included in that bin, and the threshold for the ADA was determined from an adjacent empty ocean region transform.

11.4.1 Results

The results are tabled in Table 11-2.

TABLE 11-2

NORMALIZED DIRECTIONAL SEMBLANCE RESULTS

Ocean Only
Filter D

N	Bright Wakes		Dark Wakes	
	PD	FAR	PD	FAR
4.0	-	10	-	11
4.5	-	5.9	-	9.7
5.0	-	4.8	-	6.4
5.5	-	3.2	-	5.7
6.0	-	2.0	-	3.7

Filter E

N	Bright Wakes		Dark Wakes	
	PD	FAR	PD	FAR
4.0	-	7.0	-	1.6
4.5	-	1.9	-	0.7
5.0	-	0.8	-	0.3
5.5	-	0.5	-	0.3
6.0	-	0.3	-	0.0

TABLE 11-2 (cont'd)

NORMALIZED DIRECTIONAL SEMBLANCE RESULTS

Images with Ships and Wakes
Filter D

N	Bright Wakes		Dark Wakes	
	PD	FAR	PD	FAR
4.0	.38	6.3	.31	11.4
4.5	.38	1.4	.31	5.7
5.0	.31	0.5	.23	3.3
5.5	.23	0.5	.15	3.3
6.0	.23	0.3	.15	1.9

Filter E

N	Bright Wakes		Dark Wakes	
	PD	FAR	PD	FAR
4.0	.54	5.7	.23	1.5
4.5	.46	0.8	.23	4.9
5.0	.38	0.3	.23	1.4
5.5	.38	0.3	.23	0.5
6.0	.31	0.0	.15	0.3

TABLE 11-2 (cont'd)

NORMALIZED DIRECTIONAL SEMBLANCE RESULTS

Images with Wakes Only
Filter D

N	Bright Wakes		Dark Wakes	
	PD	FAR	PD	FAR
4.0	.35	17	.18	12.5
4.5	.17	9.2	.18	8.8
5.0	.12	5.9	.18	6.8
5.5	.12	5.9	.12	5.1
6.0	.06	5.9	.12	3.7

Filter E

N	Bright Wakes		Dark Wakes	
	PD	FAR	PD	FAR
4.0	.41	9.6	.23	2.0
4.5	.24	4.1	.18	8.6
5.0	.24	2.0	.12	4.3
5.5	.18	1.0	.06	3.1
6.0	.18	0.2	.06	1.8

The results suggest some improvement in performance compared to the unnormalized semblance, for dark peaks using Filter E. The PD is increased and the empty ocean FAR is considerably reduced. Most of the empty ocean false alarms occurred in a few images, suggesting that poor matching between the ocean background and test images was responsible for these false alarms.

11.5 SEMBLANCE AND PEAK SHAPE

The bowtie_1 and bowtie_2 algorithms were applied to the peaks of the transforms that had been produced using the semblance_E filter. The output from these shape measurement algorithms was examined to see if it might be useful in differentiating wakes from false alarms. The only rule that appeared to be useful in doing this was:

Peak is a wake if D1 > 50

This rule was applied to the peaks, producing the results in Table 11-3.

TABLE 11-3

PERFORMANCE FOR SHAPE + SEMBLANCE E

	Bright Wakes		Dark Wakes	
	PD	FAR	PD	FAR
Empty Sea		0.4		0.2
Wakes Only	.47	0.0	.17	0.2
Wakes and Ships	.53	0.5	.31	0.8

12.0 CONCLUSIONS

The research has shown that a Radon Transform combined with a simple automatic peak detection algorithm can automatically detect almost all visually obvious wake components in a SAR ocean image, with a false alarm rate of much less than one false alarm per image. Wakes which are hard to detect visually also produce peaks in the transform, and can be automatically detected. To get acceptable performance for such detection more complex algorithms than the ones used in this research would be required.

The PD performances measured for the various combinations of processing do not show great differences. This is mainly because the image set used for testing the algorithms was not large enough. This lack of images also meant that the algorithms were optimized and tested on the same images, causing further uncertainty in the results. An independent set of images, the additional image set, was used for testing the baseline algorithm; the performance was similar to that on the standard image set.

Bright ship or other reflections are a hindrance to wake detection, and if possible they should be removed from the image before looking for wakes. The system performance was better for some images with the ship left in. However in these cases the ship was contributing to the wake peak in the transform, so it was the ship that was being detected. If the ship is removed then wake should be more reliably and accurately detected; such wakes could be used as confirmation that the object removed was a ship, or could be used to determine ship parameters.

The detection algorithm should take into account the variation in length between lines associated with different elements in the transform. This can be done by normalizing the transform to the line length, as was done in this research. Doing this will increase the probability of detecting wakes crossing the image near the edge.

Using statistics from empty ocean regions to adjust the peak detection algorithm parameters appears to be useful, but may be difficult to do automatically. It would be necessary to not only match the ocean area under study with a similar background, but also to ensure that the background is uniform. The ocean background appears to change significantly, even

between adjacent images, and it may be difficult to detect or compensate for this variation.

Algorithms which examine the peak shape in the transform, such as the bowtie filter, are able to differentiate wake peaks from false alarms quite reliably. The performance improvement could be translated either into increased PD or reduced FAR, by appropriate choice of thresholds in the detection algorithm.

The directional semblance filter enhanced dark wakes, and in most cases improved system performance on both bright and dark wakes. The dark wake detection improvement was expected, bright wake detections might have improved because weak bright wakes were enhanced.

The most promising combinations of techniques are:

(a) Ship removal, baseline transform, length normalization, bowtie.

(b) Ship removal, semblance E, radon transform, length normalization, and bowtie.

13.0 RECOMMENDATIONS

The research should be continued to investigate the following items.

1. A better peak detection algorithm, able to detect local peaks rather than applying an overall threshold to the image, should be developed.

2. A larger data set is necessary. A set of at least 20 images, containing 30 to 50 wake components should be used for development. The same size independent set should be used for evaluation.

3. A better method of ground truthing the images is necessary. The format should be designed for use by automatic evaluation algorithms for determining system performance.

4. The system performance should be more accurately determined. This could include allowing for multiple detections of the same wake component, using wake visibility and wake length as factors, and determining directional and positional accuracy of the detected wake.

   The evaluation algorithm should be designed for automatic, operator independent operation, both to give unbiased results and to allow efficient analysis of large amounts of data.

5. The use of peak shape detection to reduce FAR should be further examined.

6. The background ocean characteristics should be studied, so that the expected characteristics of a transform can be predicted and used in the peak detection algorithm.

7. A simple automatic ship detection algorithm should be included in the system, to remove obvious ships from the images before processing.

8. The directional semblance filter research should be continued.

9. The effect of image size on performance should be studied further; particularly to relate wake length and image size.

10. Methods of normalizing the transform to line length should be investigated. This could include direct normalization, as was done in the current study, or the use of variable line widths.

REFERENCES

Case, K. et al. "Seasat Report", The Mitre Corporation, 1984.

Cohen, Melvin and Godfried T. Toussaint. "On the Detection of Structures in Noisy Pictures", Pattern Recognition, Vol. 9, p. 95, 1977.

Colwell, R.N. (Ed.). "Manual of Remote Sensing", Vol. 1., pp. 443-474, American Society of Photogrammetry, 1983.

Deans, Stanley R. "Hough Transform from the Radon Transform", IEEE Trans. on Pattern Analysis and Machine Intelligence, PAM-3, 2, pp. 185-188, 1981.

Hammond, R.R., R.R. Buntzen, and E.E. Floren, "Using Ship Wake Patterns to Evaluate SAR Ocean Wave Imaging Mechanisms", Naval Ocean Systems Centre, 1985.

Murphy, Lesley M. "Linear Feature Detection and Enhancement in Noisy Images Via the Radon Transform", Pattern Recongition Letters 4 (1986) 279-284.

Rosenfeld, A. and A.C. Kak. "Digital Picture Processing", Vol. 1, Academic Press, 1982.

Stoffa, P.L. et al., "Direct Mapping of Seismic Data to the Domain of Intercept Time and Ray Parameter - a Plane Wave Decomposition", Geophysics Vol. 46, No. 3, pp. 255-167, March 1981.

Tunaley, James K.E. and J.B.A. Mitchell. "The Radar Image of the Turbulent Wake Generated by a Moving Ship".

Wilmut, M.J. and R.E. MacKinnon. "Ship Wake Detection in Speckle Noise Using a Modified Hough Transform", Proceedings of the Tenth Canadian Symposium on Remote Sensing, Volume 1, 1986.

APPENDIX A

IMAGE SETS

Four sets of images were used in this study, they are described here. The sets are not all independent; some of the images in the preliminary set were also used in the other three sets. The images were provided by CRC on magnetic tape, usually each image was identified by run and swath numbers. These are listed here, along with the identification number assigned to the tape on receipt by RBA.

The identification assigned to each image is listed under Image in the tables. It has the form M-x-N, where M is usually the tape number, x is the either 's' or 'v', and N is the image number from the tape. Images with an 's' (sea) are empty ocean images, images with a 'v' (vessel) contain wakes or ships.

A.1 PRELIMINARY IMAGE SET

This was a set of varying sized images. Those containing ships were usually defined so that the ship and the wake essentially filled the image; there was relatively little empty ocean area and the wake stretched along the long dimension of the image.

Image	Size	Ships	Wake Components
1-v-4	548x856	1	4
1-s-7	300x300	0	0
1-v-8	396x468	1	2
1-v-12	384x484	1	1
1-s-16	300x300	0	0
2-v-1	400x1344	1	4
2-s-2	256x256	0	0
2-v-6	500x544	1	0
2-v-10	336x856	1	3
3-v-1	420x284	1	1
3-s-3	256x256	0	0
3-v-4	512x512	2	2

A.2 SIZE OPTIMIZATION IMAGE SET

This was a set of 400x400 and 256x256 images, used in the size optimization analysis. The 256x256 images were windowed from the 400x400 images.

Image	Ships	Wake Components
1-v-4	1	3
1-v-5	1	1
1-v-11	1	3
1-v-13	1	2
2-v-1	1	3
2-v-15	1	2
3-v-24	1	1
1-s-4	0	0
1-s-5	0	0
2-s-15	0	0

A.3 STANDARD IMAGE SET

These were 400x400 images used for most of the detailed testing. These were windowed from 2048x2048 images provided by CRC. The tape, run and swath numbers refer to the identification on the original tapes.

Tape 9 Run 66 swath E

Image	offset in full 2048x2048 image		Number of Ships	Number of Wake Components
	Col	Row		
9-s-1	0,	0	0	0
9-s-2	920,	240	0	0
9-s-3	0,	1444	0	0
9-s-4	1648,	1624	0	0
9-v-1	800,	800	1	2
9-v-2	800,	1025	0	2
9-v-3	484,	244	1	1
9-v-4	484,	344	0	1

Tape 10 Run 28, swath E.

Image	offset in full 2048x2048 image		Number of Ships	Number of Wake Components
	Col	Row		
10-s-1	564	64	0	0
10-s-2	1452	64	0	0
10-s-3	940	612	0	0
10-s-4	1648	1624	0	0
10-v-1	1	140	1	2
10-v-2	88	416	0	2
10-v-3	208	654	1	2
10-v-4	256	1626	0	1
10-v-5	1168	1398	1	2
10-v-6	1200	1279	0	2

(There were 3 ships in the original image. Image 10-v-2 contains wake components from two of them)

Tape 11 Run 28, swath E.

Image	offset in full 2048x2048 image		Number of Ships	Number of Wake Components
	Col	Row		
11-s-1	1230	1640	0	0
11-s-2	1200	1024	0	0
11-s-3	720	1024	0	0
11-s-4	800	1400	0	0
11-v-1	320	1280	0	3
11-v-2	0	960	0	3
11-v-3	192	320	1	4
11-v-4	0	1360	0	3

There were only minor overlaps in these images. 11-v-3 has a possible ship in it, the others show no obvious bright ship.

A.4 ADDITIONAL IMAGE SET

These were additional 400x400 images provided by CRC.

Image	Run	Number of Ships	Number of Wake Components
17-s-1	20	0	0
17-s-2	28	0	0
17-s-3	46	0	0
17-s-4	86	0	0
18-s-2	50	0	0
16-v-1	20	1	2
16-v-2	46	1	4
16-v-3	28	1	2
16-v-4	28	1	1
16-v-5	28	1	2
16-v-6	28	1	1
16-v-7	86	1	1
18-v-1	50	1	1
18-v-3	66	1	1
18-v-4	66	1	3
18-v-5	66	1	0

APPENDIX B

RADON TRANSFORM ALGORITHM

```
Create a blank transform array, f(s,t), with
n columns and m rows, where m is a user-defined
number of radius intervals, n the user-defined
number of angle intervals.

FOR each pixel g(i,j)  in the input image

   FOR the central angle, t, in each angle interval

      Calculate p = x cos(t) + y sin(t)

      Find k and l such that p falls into radius
       interval k, and t falls into angle interval l.

      Add W*(g(i,j) - g_normal) to the bin f(l,k),
       where W is a multiplicative normalization
       constant and g_normal an additive normalization
       constant, both user defined.

   END FOR

END FOR
```

APPENDIX C

IMAGES

This Appendix shows some original Seasat wake images, results of some of the preprocessing filters applied to these images, and various types of Radon transforms used in the analysis. The processing done for each image is briefly described in the captions, reference is made to the appropriate section of the text for a fuller explanation.

These images are all presented as pseudo-colour images, that is each grey level in the original image is displayed as a different colour. When captions refer to regions with a particular brightness the colour associated with the brightness is given in parentheses.

The grey level scale is the same for the two original Seasat images shown, since they were both compressed from the original data in the same way (section 2.1). The grey level scales generally differ between Radon transforms, since each transform was linearly compressed so that the brightest element was at grey level 255, and the darkest was at grey level 0 (section 3.2).

The images shown are all 400x400 pixels in size; the transforms are all 256x256 pixels. Most of the transforms are of image 9-V-1, which was chosen as a representative image with some strong features that showed clearly in the transform.

Plate 1: Image 9-V-1

A pseudo-colour representation of a Seasat SAR image, showing a 10km by 10 km area. The scale indicates the relationship between image grey level and pseudo-colour. The bright (blue) reflections at the intersection of the wake arms are produced by the ship. The turbulent wake is the bright (blue) line directly behind the ship, a second (yellow) set of arms is also visible to the left of the turbulent wake. The turbulent wake in this image was one of the brightest components in the image sets studied.

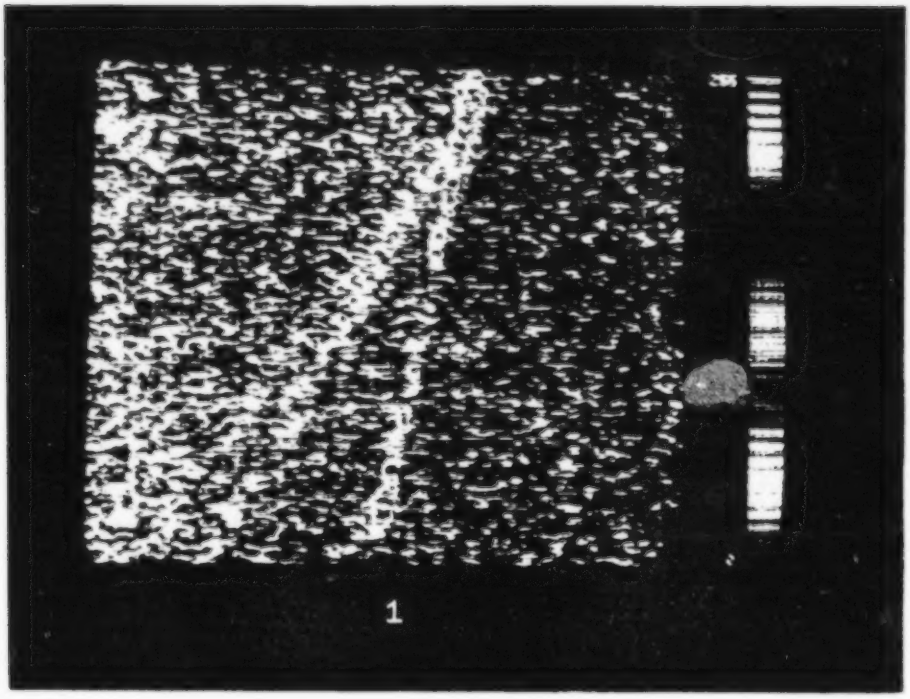
1

Plate 2: Baseline Radon Transform of Image 9-V-1

A pseudo-colour representation of a 256x256 transform of the image in plate 1, (section 8). The labels indicate the radius and angle coordinates. The maximum radius is 565, representing the longest possible line in a 400x400 image. The bright peak at 1 is due to the turbulent wake; there is a small peak at 2, produced by the arms on the left side of the wake. The baseline automatic detection algorithm (ADA), (section 8.3), correctly detected peak 1. Peak 2 was not detected as it was combined with peak 1 (section 8.4). The 'bowtie' shape of peak 1 (section 10.2) can be clearly seen.

Plate 3: Radon Transform of Image 9-S-3

The transform of an ocean region adjacent to image 9-V-1. The transform was originally compressed to a range of 0 to 255, it has been rescaled to the compression used for transform 9-V-1, so colours on the two plates are directly comparable. It can be seen that the transforms are similar except for the bright sinusoidal lines produced by the bright ship and wake pixels in plate 2.

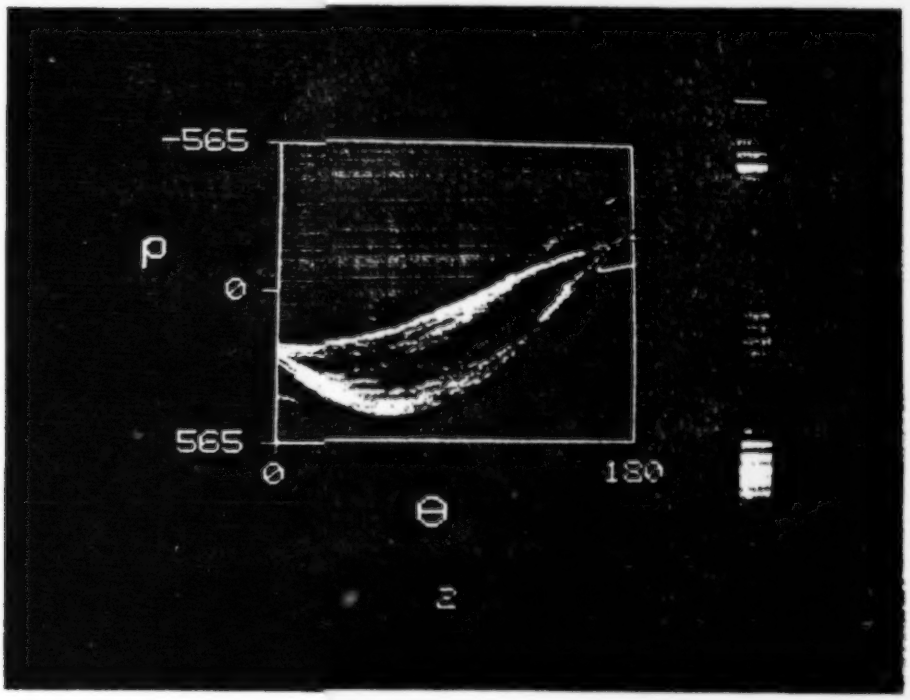
-565
ρ
0
565
0
180
θ
2

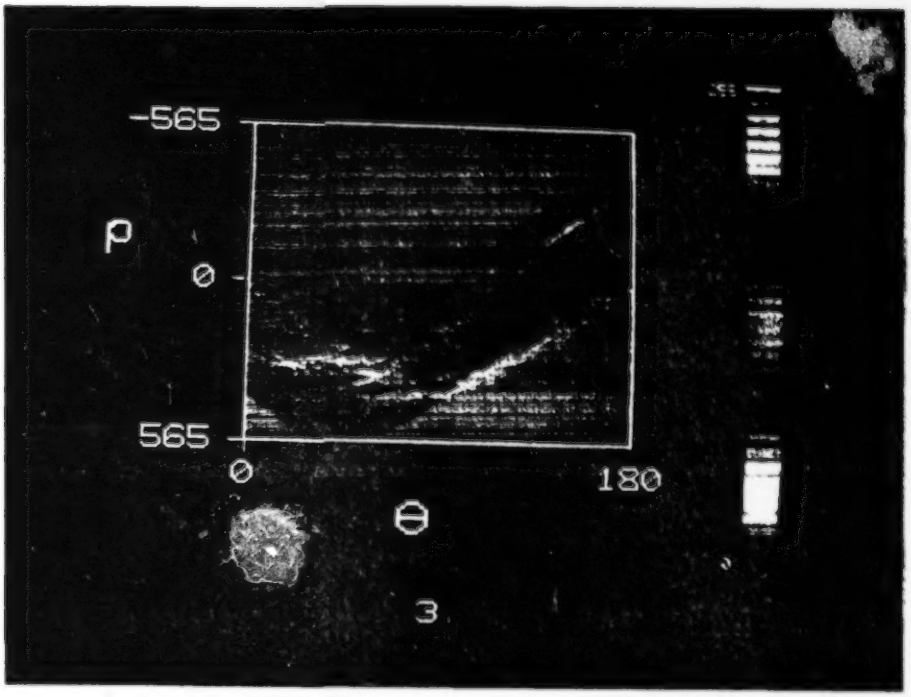
-565
ρ
0
565
0
180
θ
3

Plate 4: Image 10-V-1

The image shows a ship producing two adjacent wake components. The ship is the bright (blue) area near the top left. Component 1 is dark (orange) and clearly visible behind the ship. Component 2 is immediately to the left of 1, and is barely visible. It cannot be identified as bright or dark, although it contains some bright (green) regions.

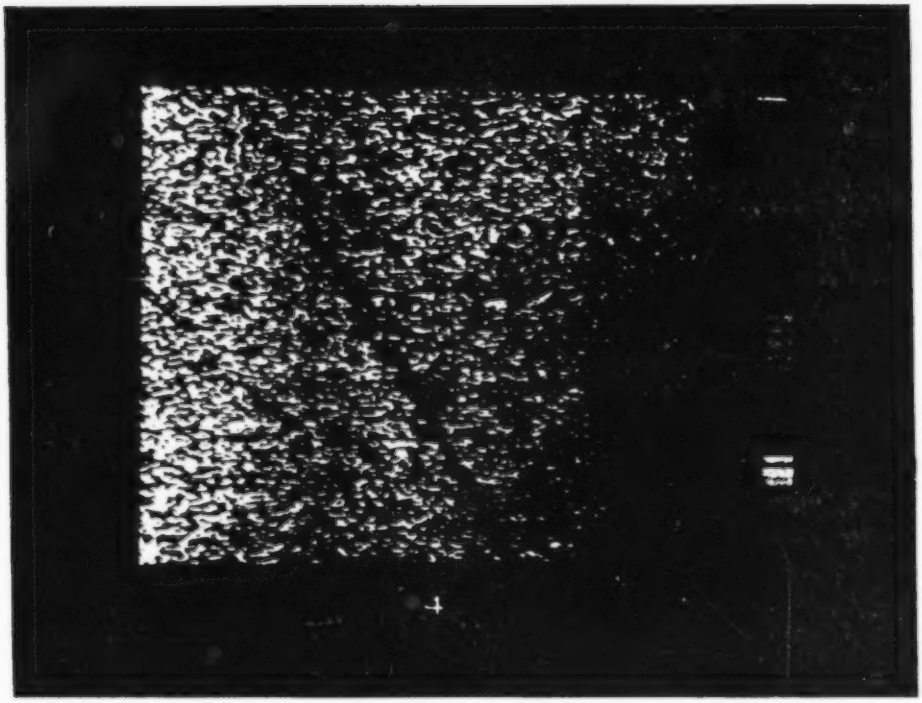

Plate 5: Radon Transform of Image 10-V-1

The dark (yellow) peak at 1 is due to the dark wake, component 1, in image 10-V-1.

The bright (violet) line next to it, labelled 2, is due to the bright ship pixels, it is not present in the 10-V-2 transform (plate 6, below). It is evident from this that the ship reflections may overpower those due to wakes.

The automatic detection algorithm (ADA) detected component 1 as a dark wake and component 2 as a bright wake.

Plate 6: Baseline Radon Transform of image 10-V-2

Image 10-V-2 consists of the wake portion of image 10-V-1, it does not include the region containing the ship.

The dark (orange) peaks 1 and 2 are due to wake components 1 and 2. They were both detected as dark peaks by the ADA.

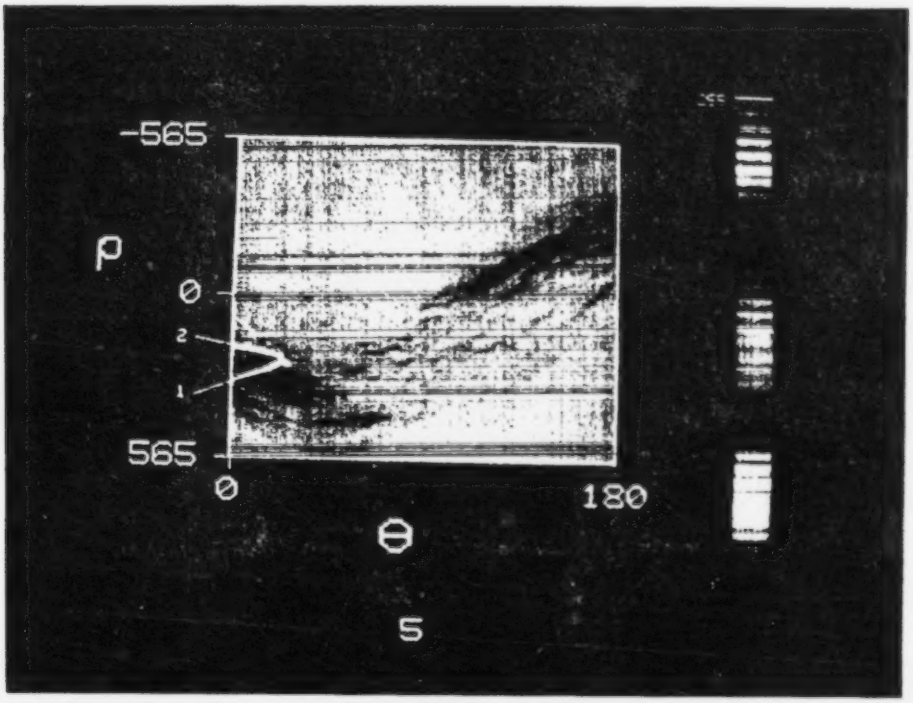
-565
p
0
2
1
565
0
180
θ
5

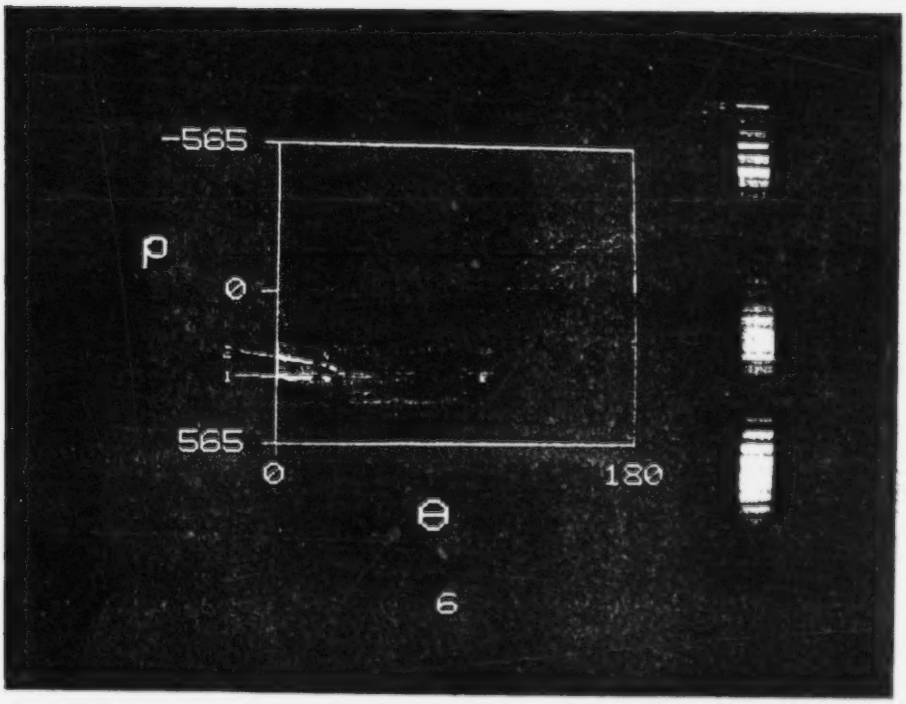
-565
p
0
2
1
565
0
180
θ
6

Plate 7: Line Lengths in a Transform

The figure was produced by taking the Radon transform of an image with a constant grey level of 1. Each transform element brightness is thus proportional to the length of the associated image line. The transform was used to normalize image transforms to the line length (section 9).

Plate 8: `Normalized Transform of Image 9-V-1

The transform shown in plate 2, normalized to the line length (section 9). The peaks are still clearly visible, but the variation in brightness due to line length variation has been removed.

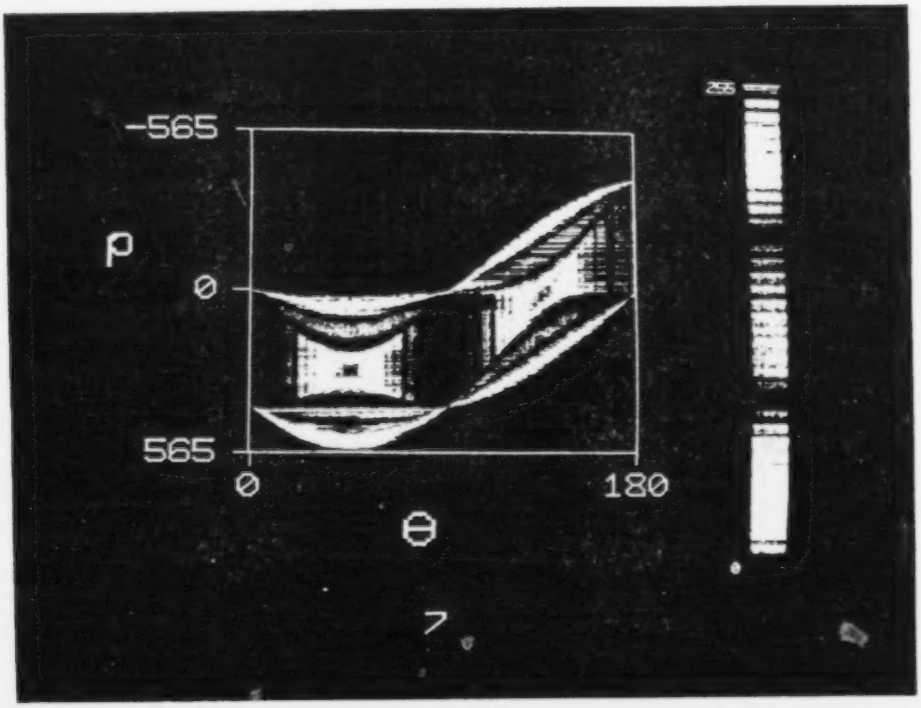
-565
p
0
565
0
180
θ
255
7

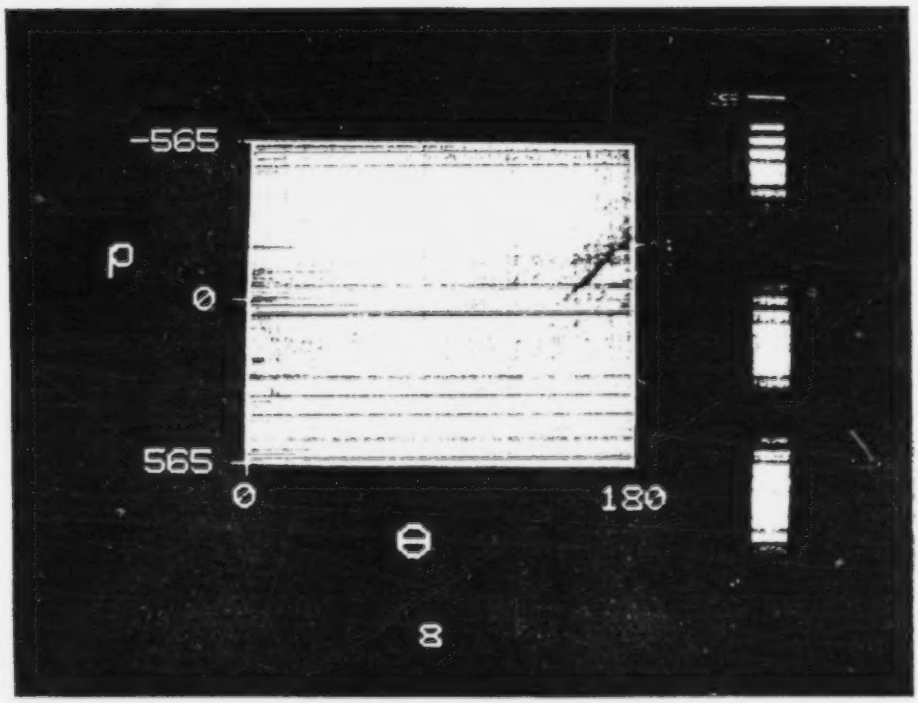
-565
p
0
565
0
180
θ
8

Plate 9: 3x3 Semblance of Image 9-V-1

The output of the 3x3 semblance filter pre-processor (section 11.1) applied to the image. The semblance measures the uniformity of a region in the input image. In this case it is taken over a 3x3 window around each pixel of the original window. The semblance is 1 for uniform regions, 0 for regions of high variation; it has been rescaled to a range of 0-255 in these images. The bright wake is still visible, but is considerably degraded compared to the original image in plate 1.

Plate 10: Slant Stack Transform of Image 9-V-1

The slant stack transform (section 11.2) measures the semblance along each line in the Radon transform. This transform shows the bright peak due to the turbulent wake. The peak is lower and less visible than in the baseline transform seen in plate 2. The bright spots on the edge of the transform are due to lines containing only a few uniform pixels, with a semblance close to 1.

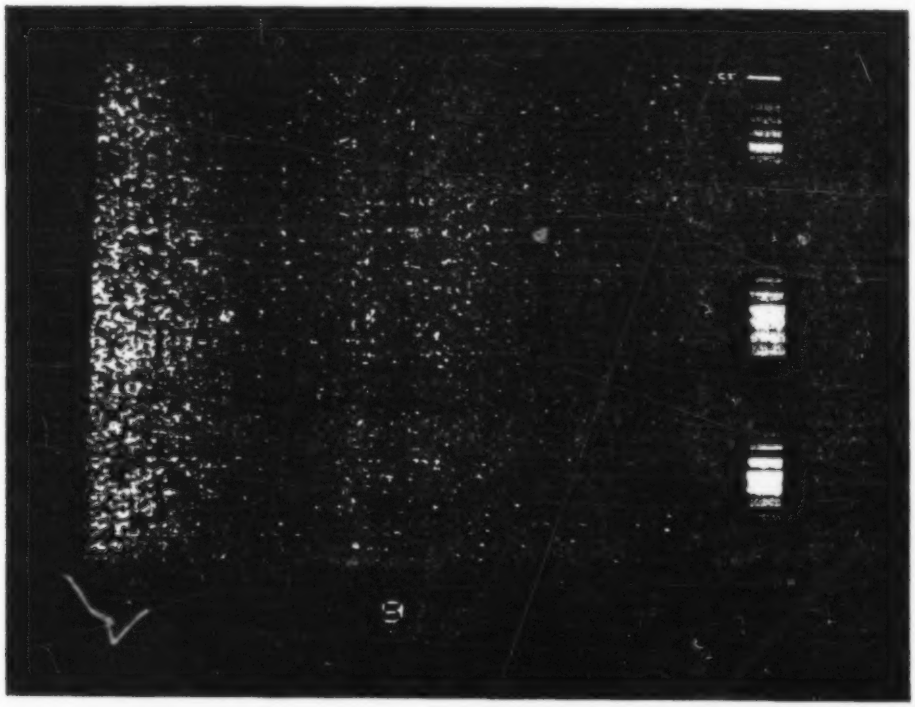
9

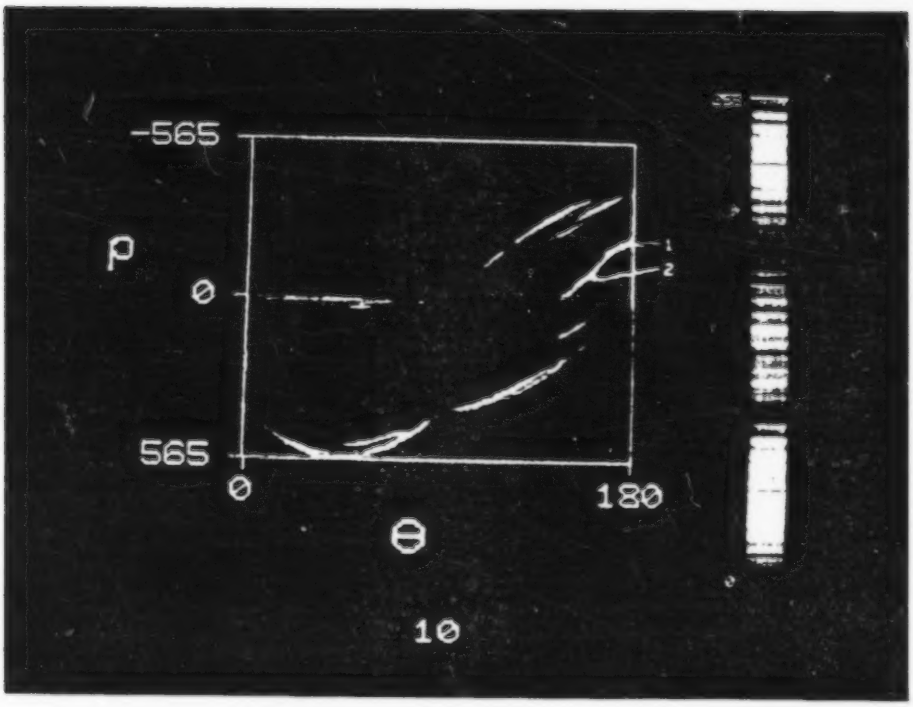
-565
p
0
565
0
180
θ
1
2
10

Plate 11: Directional Semblance Filter E on Image 9-V-1

The directional semblance (section 11.3) is measured along short lines through each pixel in 4 different directions. The four output images from directional semblance filter E are shown in a, b, c, and d. Each output image emphasizes linear features in a particular direction.

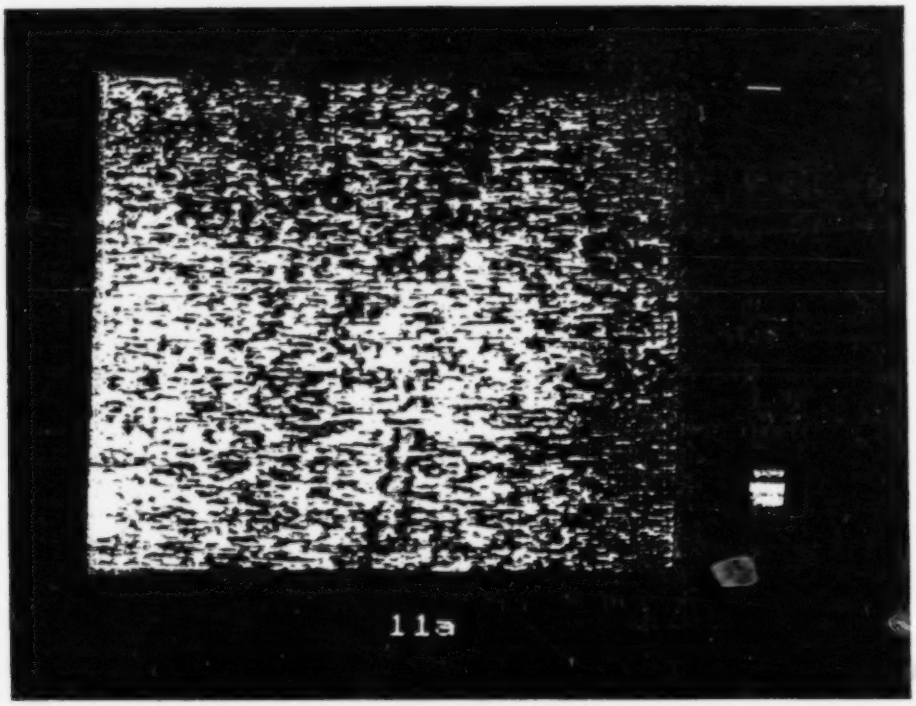

11a

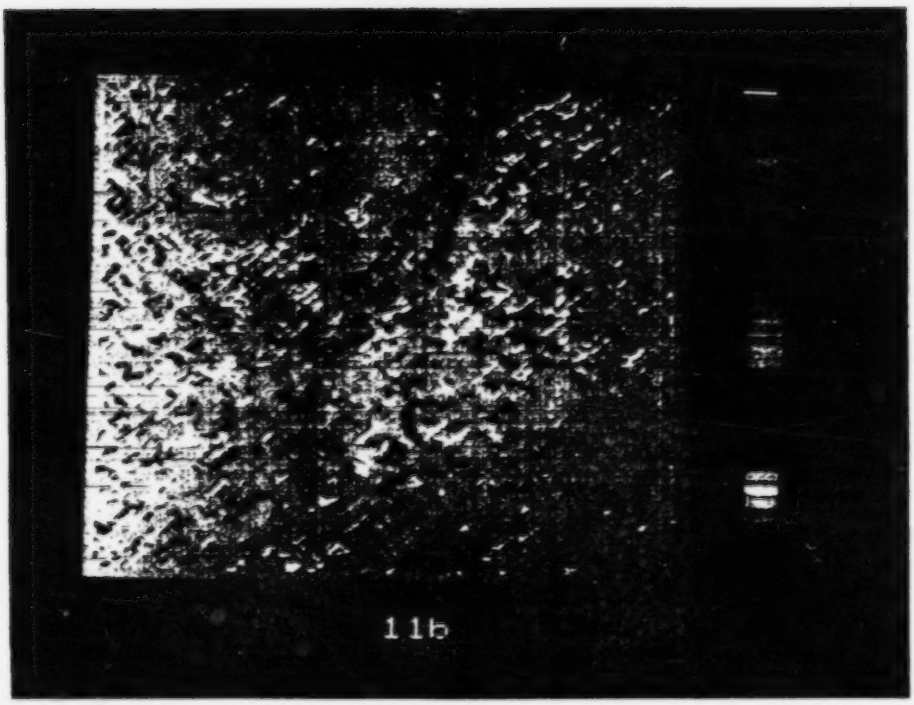

11b

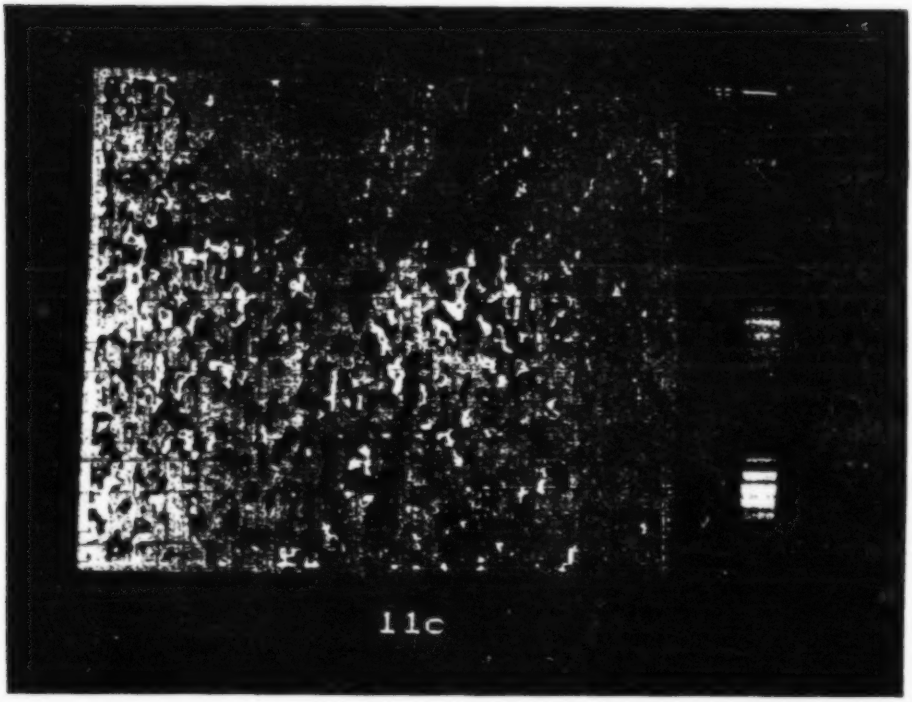

11c

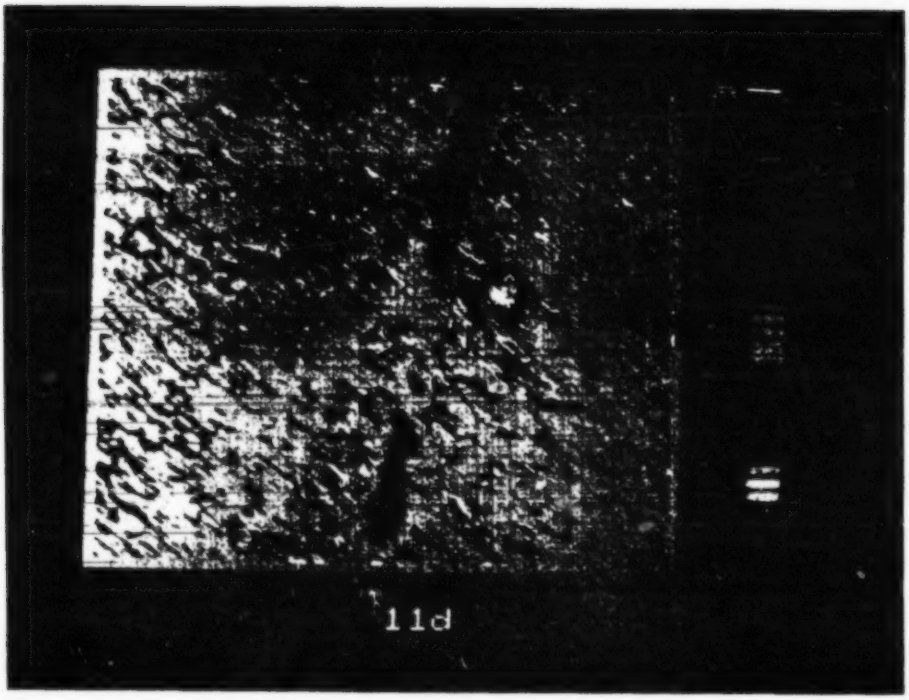

11d

Plate 12: Directional Semblance Filter Radon Transform

The filtered images in plate 11 were transformed, and then combined as described in section 11.3, to produce this result. The peaks due to the two wake components are clearly visible.

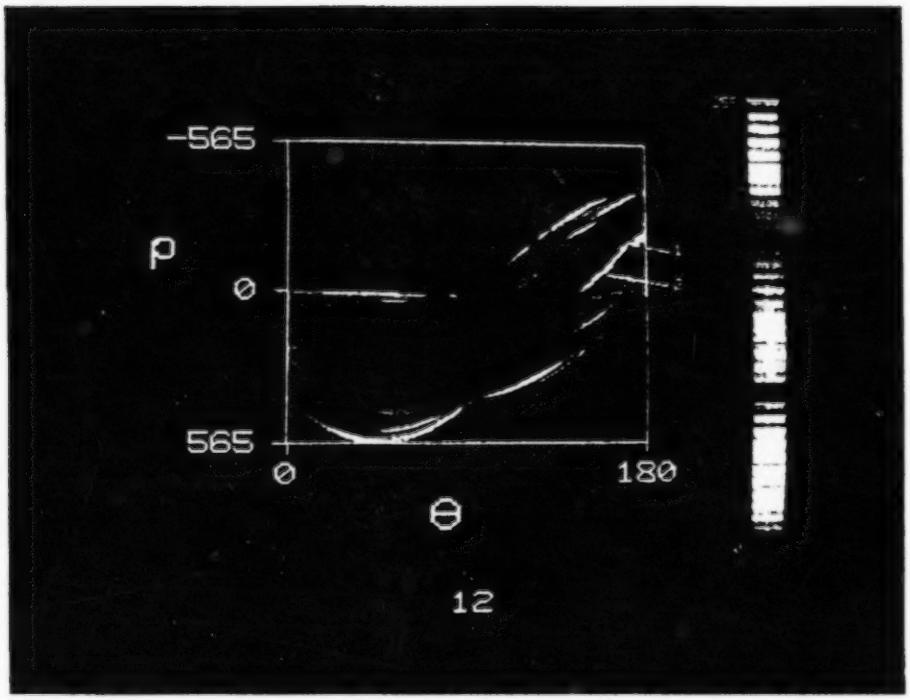
-565
P
0
565
0
180
θ
12

SECURITY CLASSIFICATION OF FORM
(highest classification of Title, Abstract, Keywords)

DOCUMENT CONTROL DATA

(Security classification of title, body of abstract and indexing annotation must be entered when the overall document is classified)

1. ORIGINATOR (the name and address of the organization preparing the document. Organizations for whom the document was prepared, e.g. Establishment sponsoring a contractor's report, or tasking agency, are entered in section 8.)

Roy Ball Associates Ltd.
1750 Courtwood Crescent
Ottawa, Ontario K2C 2B5

2. SECURITY CLASSIFICATION (overall security classification of the document. including special warning terms if applicable)

Unclassified

3. TITLE (the complete document title as indicated on the title page. Its classification should be indicated by the appropriate abbreviation (S,C,R or U) in parentheses after the title.)

Radon Transform Techniques for Wake Detection in SAR Images (U)

4. AUTHORS (Last name, first name, middle initial. If military, show rank, e.g. Doe, Maj. John E.)

Folinsbee, James T.
Ball, Roy D.

5. DATE OF PUBLICATION (month and year of publication of document)

March 1988

6a. NO. OF PAGES (total containing information. Include Annexes, Appendices, etc.)

118

6b. NO. OF REFS (total cited in document)

10

7. DESCRIPTIVE NOTES (the category of the document, e.g. technical report, technical note or memorandum. If appropriate, enter the type of report, e.g. interim, progress, summary, annual or final. Give the inclusive dates when a specific reporting period is covered.)

Final Technical Report

8. SPONSORING ACTIVITY (the name of the department project office or laboratory sponsoring the research and development. Include the address.)

Defence Research Establishment Ottawa
Shirley Bay, Ottawa, K1A 0Z4

9a. PROJECT OR GRANT NO. (if appropriate, the applicable research and development project or grant number under which the document was written. Please specify whether project or grant)

9b. CONTRACT NO. (if appropriate, the applicable number under which the document was written)

W7714-6-5226/01-SV

10a. ORIGINATOR'S DOCUMENT NUMBER (the official document number by which the document is identified by the originating activity. This number must be unique to this document.)

FR-C250-000-0000

10b. OTHER DOCUMENT NOS. (Any other numbers which may be assigned this document either by the originator or by the sponsor)

11. DOCUMENT AVAILABILITY (any limitations on further dissemination of the document, other than those imposed by security classification)

(X) Unlimited distribution
( ) Distribution limited to defence departments and defence contractors; further distribution only as approved
( ) Distribution limited to defence departments and Canadian defence contractors; further distribution only as approved
( ) Distribution limited to government departments and agencies; further distribution only as approved
( ) Distribution limited to defence departments; further distribution only as approved
( ) Other (please specify):

12. DOCUMENT ANNOUNCEMENT (any limitation to the bibliographic announcement of this document. This will normally correspond to the Document Availability (11). However, where further distribution (beyond the audience specified in 11) is possible, a wider announcement audience may be selected.)

SECURITY CLASSIFICATION OF FORM

13. ABSTRACT (a brief and factual summary of the document. It may also appear elsewhere in the body of the document itself. It is highly desirable that the abstract of classified documents be unclassified. Each paragraph of the abstract shall begin with an indication of the security classification of the information in the paragraph (unless the document itself is unclassified) represented as (S), (C), (R), or (U). It is not necessary to include here abstracts in both official languages unless the text is bilingual).

A system to automatically detect ship wakes in synthetic aperture radar ocean images has been developed. The basic system does the Radon transform of the SAR image, then detects bright and dark peaks produced in the transform by wakes in the image. It was tested on a set of 26 400x400 Seasat images; it had a probability of detection (PD) of 0.46 for individual wake components, and a false alarm rate (FAR) of 9 alarms per 512x512 area. It detected at least one wake component for every ship in the images.

A number of additional processing techniques were developed and tested, including normalizing the Radon transform to image line length, automatically analyzing the shape of the peaks in the transform, and applying various semblance filters to the image. The most successful were the shape detection and directional semblance. Shape detection reduced FAR to 0.5, without affecting PD. The directional semblance increased dark wake peak heights by up to 50%, and increased PD from .23 to .31 for dark wake components.

14. KEYWORDS, DESCRIPTORS or IDENTIFIERS (technically meaningful terms or short phrases that characterize a document and could be helpful in cataloguing the document. They should be selected so that no security classification is required. Identifiers, such as equipment model designation, trade name, military project code name, geographic location may also be included. If possible, keywords should be selected from a published thesaurus, e.g. Thesaurus of Engineering and Scientific Terms (TEST) and that thesaurus identified. If it is not possible to select indexing terms which are Unclassified, the classification of each should be indicated as with the title.)

Seasat, Synthetic Aperture Radar, Radon Transform, Semblance, Wakes, Linear Feature, Ship, Ocean

SECURITY CLASSIFICATION OF FORM

Defence Research and Development Canada | Recherche et développement pour la défense Canada | Canada

Français Contact Us Help Search Canada Site
Home Defence R&D Canada Defence Site

Browse Indexes
Titles
Authors
Descriptors
Corporate Authors
Corporate Acronyms
Report Numbers
Search Database
Summary

It is recommended you search "Authors" and "Corporate Authors" on their respective "Browse" pages.

Click here if you are having problems displaying text (ie. text is too big, or too small) or page appears to be jumbled.

Prior Top **Document:** 250 of 394 Bottom Next Click here to Order Click here to Download

TITLE:(U) RADON TRANSFORM TECHNIQUES FOR WAKE DETECTION IN SAR (SYNTHETIC APERTURE RADAR) IMAGES

PERSONAL AUTHOR: Folinsbee, J.T.; Ball, R.D.
CORPORATE AUTHOR: Roy Ball Associates Ltd, Ottawa ONT (CAN);Defence Research Establishment Ottawa, Ottawa ONT (CAN)

ABSTRACT: (U) A system to automatically detect ship wakes in synthetic aperture radar ocean images has been developed. The basic system does the Radon transform of the SAR image, then detects bright and dark peaks produced in the transform by wakes in the image. It was tested on a set of 26 400x400 Seasat images; it had a probability of detection (PD) of 0.46 for individual wake components, and a false alarm rate (FAR) of 9 alarms per 512x512 area. It detected at least one wake component for every ship in the images.

DESCRIPTORS: (U) Synthetic aperture radar;Radar images;Ships;Ocean environments;Wakes;Wake detection;Signal processing;Surface targets;Target acquisition;SEASAT;Image processing

REPORT NUMBER: FR-C250-000-0000; Contractor Report (Final)
REPORT DATE: 15 Mar 1988
NUMBER OF PAGES : 119
DRDKIM N°: 89-00422
CANDIS N°: 58364
Format(s): Hardcopy;Originator's fiche received by DSIS;Document Image stored on Optical Disk

Date modified: 2003-04-17 Important Notices